ARMY RESEARCH LABORATORY

System Tests of Optimized (2nd Pass) Gallium Arsenide (GaAs) Integrated Circuit Radio Frequency (RF) Booster Designs for 425 MHz and Dual Band (425 and 900 MHz)

by John E. Penn

ARL-TR-5749 **September 2011**

NOTICES

Disclaimers

The findings in this report are not to be construed as an official Department of the Army position unless so designated by other authorized documents.

Citation of manufacturer's or trade names does not constitute an official endorsement or approval of the use thereof.

Destroy this report when it is no longer needed. Do not return it to the originator.

Army Research Laboratory
Adelphi, MD 20783-1197

ARL-TR-5749 **September 2011**

System Tests of Optimized (2nd Pass) Gallium Arsenide (GaAs) Integrated Circuit Radio Frequency (RF) Booster Designs for 425 MHz and Dual Band (425 and 900 MHz)

John E. Penn
Sensors and Electron Devices Directorate, ARL

REPORT DOCUMENTATION PAGE

Form Approved
OMB No. 0704-0188

1. REPORT DATE *(DD-MM-YYYY)*	2. REPORT TYPE	3. DATES COVERED (From - To)
September 2011	Final	

4. TITLE AND SUBTITLE
System Tests of Optimized (2nd Pass) Gallium Arsenide (GaAs) Integrated Circuit Radio Frequency (RF) Booster Designs for 425 MHz and Dual Band (425 and 900 MHz)

5a. CONTRACT NUMBER

5b. GRANT NUMBER

5c. PROGRAM ELEMENT NUMBER

6. AUTHOR(S)
John E. Penn

5d. PROJECT NUMBER

5e. TASK NUMBER

5f. WORK UNIT NUMBER

7. PERFORMING ORGANIZATION NAME(S) AND ADDRESS(ES)
U.S. Army Research Laboratory
ATTN: RDRL-SER-E
2800 Powder Mill Road
Adelphi, MD 20783-1197

8. PERFORMING ORGANIZATION REPORT NUMBER
ARL-TR-5749

9. SPONSORING/MONITORING AGENCY NAME(S) AND ADDRESS(ES)

10. SPONSOR/MONITOR'S ACRONYM(S)

11. SPONSOR/MONITOR'S REPORT NUMBER(S)

12. DISTRIBUTION/AVAILABILITY STATEMENT
Approved for public release; distribution unlimited.

13. SUPPLEMENTARY NOTES

14. ABSTRACT
High-performance microwave and radio frequency integrated circuits are of interest to the Army. The radio frequency (RF) integrated circuit (RFIC) booster chip is intended to increase range between RF nodes for low-power wireless applications. The booster concept uses the excellent RF performance advantages of gallium arsenide (GaAs) and is easily inserted into systems based on commercial silicon (Si) RFIC transceivers to enhance their capabilities and improve size, weight, and power (SWAP). This report documents these system-level tests showing the performance enhancements possible by combining a simple custom GaAs RFIC design with wireless systems based on commercial-off-the-shelf (COTS) transceivers.

15. SUBJECT TERMS
monolithic microwave integrated circuit, RFIC, RF

16. SECURITY CLASSIFICATION OF:			17. LIMITATION OF ABSTRACT	18. NUMBER OF PAGES	19a. NAME OF RESPONSIBLE PERSON
a. REPORT	b. ABSTRACT	c. THIS PAGE			John E. Penn
Unclassified	Unclassified	Unclassified	UU	58	19b. TELEPHONE NUMBER (*Include area code*) (301) 394-0423

Contents

List of Figures

List of Tables

1. Introduction

Increased transmission range in low-power radio frequency (RF) applications is desirous for the U.S. Army. The RF integrated circuit (RFIC) booster chip is intended to increase range between RF nodes for low-power wireless applications. The booster concept uses the excellent RF performance advantages of the gallium arsenide (GaAs) process to enhance the capabilities of systems using commercial silicon (Si) RFIC transceivers. It can be inserted easily into systems to increase transmit power, receiver sensitivity, and efficiency or battery usage. A 2nd pass tile of optimized RFIC designs were designed and fabricated, improving the RF performance based on results of a set of 1st pass designs. The second tile set also included passive matching IC designs to extend the integration and improve size, weight, and power (SWAP) (i.e., reduce the board area). Previously, the passive matching circuits were only tested at the die level with a probe station, as they require an RFIC system in order to complete more extensive testing. Some of these passive 2nd pass designs were tested with a commercial wireless development system. Additionally, the active 2nd pass RF designs were tested at a system level to demonstrate the enhanced performance (i.e., range potential) using a commercial wireless development system. This report documents these system-level tests showing the performance enhancements possible by combining a simple custom GaAs RFIC design with wireless systems based on commercial-off-the-shelf (COTS) transceivers.

2. Summary of 2nd Pass Designs Used for System Tests

The Booster IC concept illustrates the performance advantages possible in heterogeneous integration by combining the technologies of a Booster IC using the RF performance advantages of GaAs technology with a COTS-based Si RF transceiver using the low-cost, low-power, large-scale digital integration of Si. While the concept can be extended to a broad range of wireless communications, IC technologies, and frequencies, this work's focus was predominantly the 400–450 MHz frequency band, with an additional extension to a broadband or dual-band capability (400/900 MHz). See references 1 to 8 for previous Booster IC documentation.

Some of the circuits of the 2nd pass GaAs tile design were passive matching circuits intended for use with common COTS RFIC circuits. These passive integrated circuits were designed to reduce SWAP at the system- or board-level design. The COTS parts targeted were the Texas Instruments (TI) CC1000 transceiver and the newer CC1100 transceiver, which includes an internal MSP430 microcontroller. These two commercial RFICs are capable of operating up to 1 GHz but require external matching elements, which typically limit the operating band of the system design. The matching circuits demonstrated in this system test include two ICs designed

for the 425-MHz band with the CC1100 series RFIC, one for a single RF connection (i.e., antenna) and the second with two switched RF connections (i.e., in and out for use with the active Booster IC design). A second dual-band IC designed to switch between the 425 and 900 MHz bands with the CC1100 series RFIC includes two switched RF connections. Since future wireless designs would use the newer CC1100 part rather than the older CC1000 part, the passive matching circuits intended for demonstration with the older CC1000 RFIC were not tested in these system level tests (see previous die-level tests, reference 7).

In the 2nd pass GaAs tile fabrication, there were four active design variations targeting 50 mW at 2.8 V, 100 mW at 2.8 V, around 50 mW for 2.8 V to 3.6 V operation, and a dual-band design at 425 and 900 MHz. All four of the active designs were tested with a TI CC11XX Chronos wireless development kit. Tests were performed at 433 and 915 MHz using two different Chronos systems and its RF access point designs.

3. Use of TI Chronos RF Access Point for System Tests

The U.S. Army Research Laboratory's (ARL) Booster IC is also being tested by a system integrator with their modified (tagging, tracking, and locating [TTL]) tag to prove out the design and concept with an existing fielded wireless tag. That work is being done in parallel and will be documented by the system integrator. Meanwhile, the TI eZ430-Chronos development kit was used for ARL's own system-level tests with the Booster ICs and is documented in this technical report.

The eZ430-Chronos development kit consists of a wireless watch component, a universal serial bus (USB)-based programmer board for developing application code for the wireless watch, and a simple RF access point for wireless communication between the watch component and a USB enabled computer. The RF access point provided an ideal vehicle for demonstrating and testing the Booster IC designs in a wireless system. Chronos development kits were obtained for both the 433- and 915-MHz bands. Figure 1 shows a photo of a typical RF access point board, which consists of a TI CC1111F32 RFIC transceiver complete with a USB interface and a MSP430 microcontroller. Additional discrete components and a chip antenna make up the rest of the required components for the system to wirelessly communicate to and from the wireless CC11XX-based watch.

Figure 1. The 915-MHz RF access point photo 14x45 mm (from the TI Chronos User's Guide).

The Booster IC is intended to be easily inserted into an existing wireless system to extend the range and performance of the COTS-based system. This is an ideal demonstration of that concept, showing that existing application code and IP for the COTS part can be reused. Extended transmission range is easily demonstrated by removing the chip antenna of the existing part, inserting connection to the active Booster IC, and then connecting the output of the Booster IC to an antenna or test instrument. Demonstrating the ability to integrate matching circuits into a custom integrated IC requires removing the existing discrete lumped element components and inserting the passive Booster ICs directly tied to the two unmatched RF pins of the CC11XX transceiver.

4. Simple Printed Circuit (PC) Board to Test the 433-MHz Matching IC (ARL29M425)

A simple printed circuit (PC) board was created to test the ARL29M425 Booster IC and the similar ARL29M425S, which contains switches to split the single antenna bidirectional connection to an RF input and output for direct use with the active Booster IC designs, which have separate single-ended RF connections for transmit and receive. Figure 2 shows the simple schematic of the board design using ExpressPCB software. The top part of the schematic shows the dual RF differential connections to the CC11XX RFIC and the single antenna output connection for the ARL29M425 matching circuit. The bottom portion shows the connections for the dual RF differential connections to the CC11XX RFIC, the two control switch inputs, and the two RF connections for the transmit and receive paths of the ARL29M425S matching circuit. Figure 3 shows the simple two-sided board layout of the test board, which overlays the RF access point board, replacing its discrete matching components.

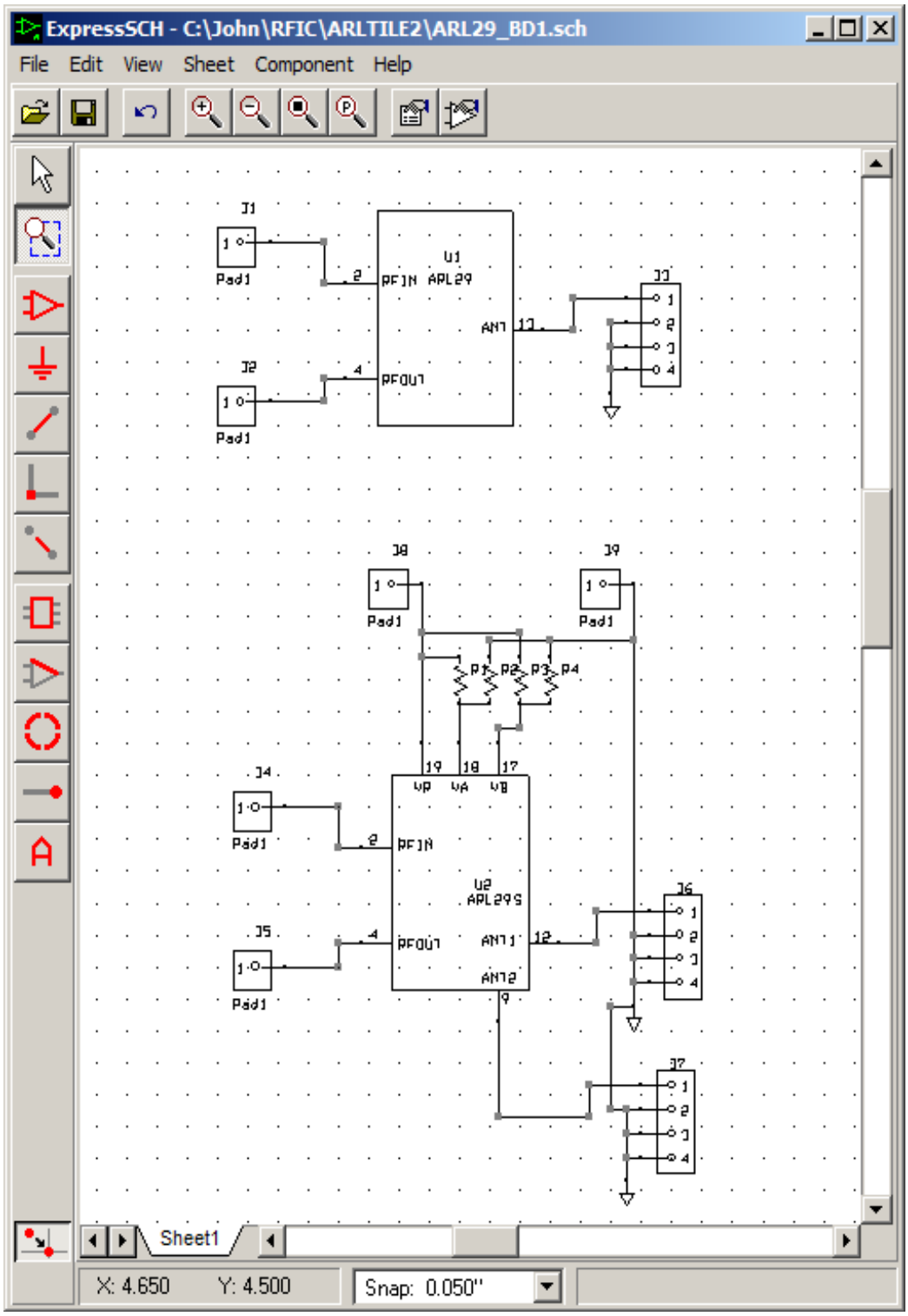

Figure 2. Schematic of the ARL29 integrated matching RF circuit test PC board.

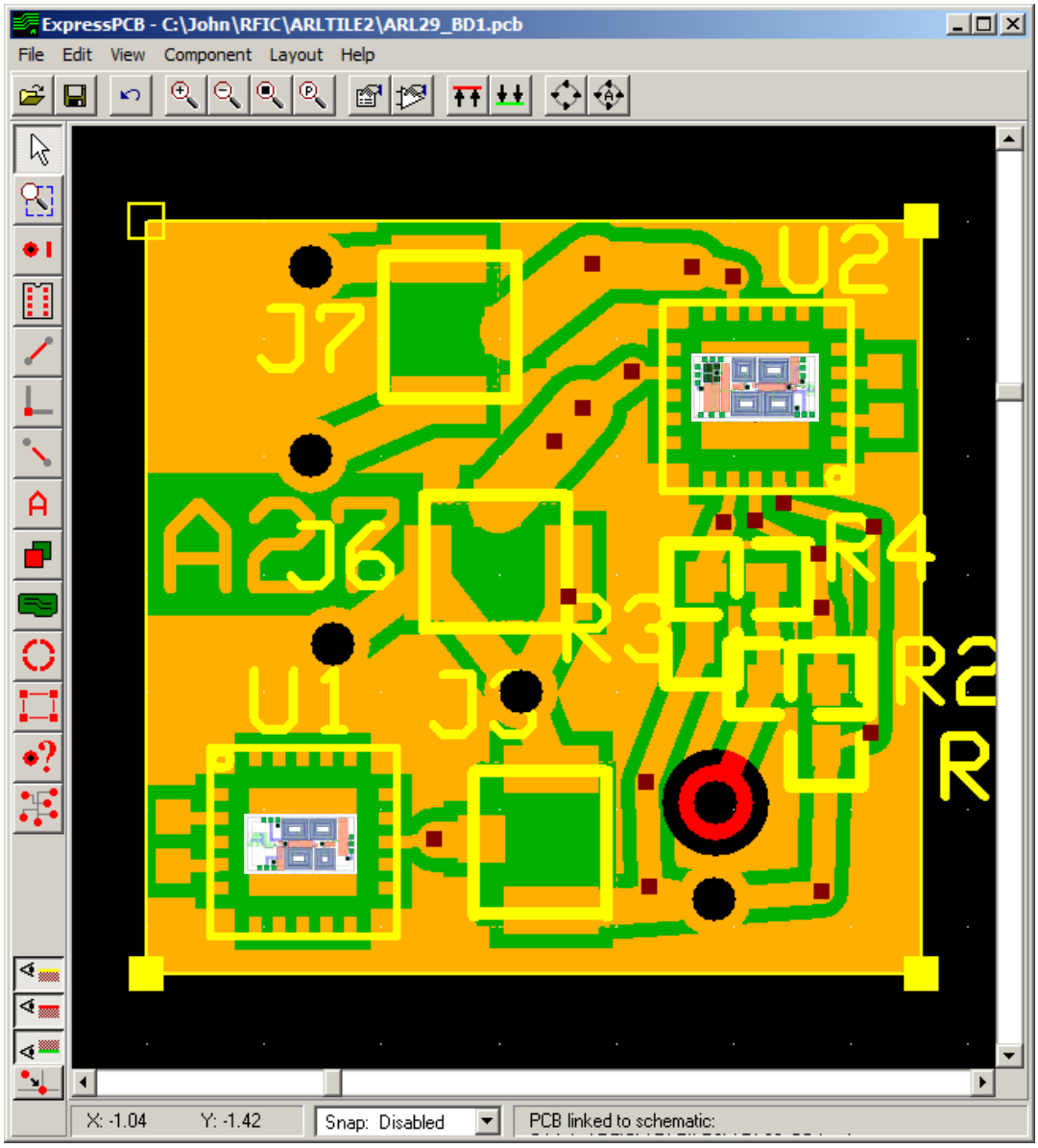

Figure 3. Layout of the ARL29 integrated matching RF circuit test PC board.

The bottom portion of the PC board has the ARL29M425 IC (U1) in a 4x4 mm quad flat no leads (QFN) package with its RF output connected to a small UFL RF connector (J3). To test the matching circuit IC, the discrete matching components L2, L3, C16, and C17 plus the chip antenna are removed (figure 4). The test board is attached to the RF access point board and short wire connections are made to the two RF connections of the CC1111 RFIC (L3, C17 pads). Figure 5 shows a photo of the actual assembled test board and RF access point PC board. Figure 6 shows the wire bonding of the 50x95 mil ARL29M425 die in a 4x4 mm QFN package. At these ultra-high frequencies (UHF), the low wire bond inductances have little effect on the RF performance.

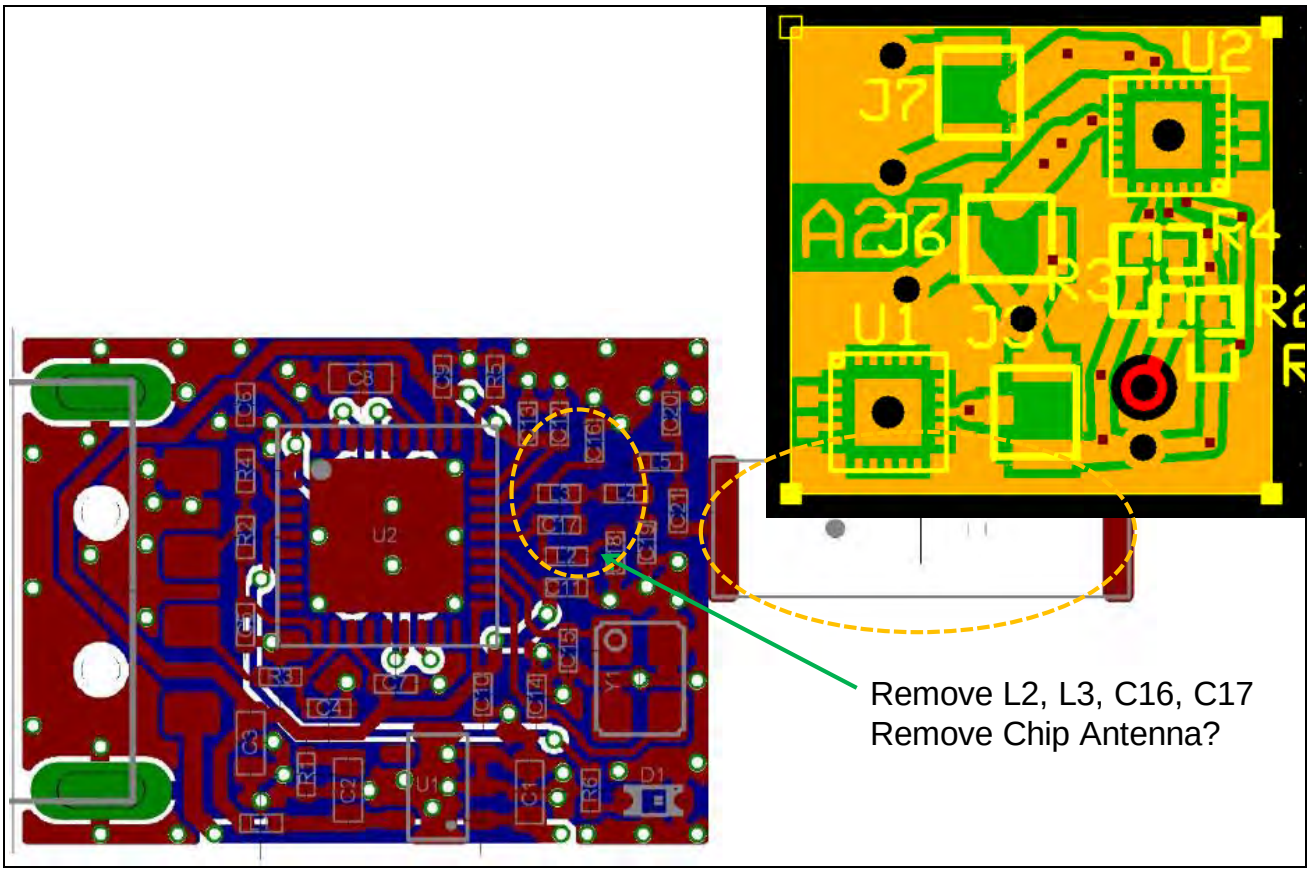

Figure 4. ARL29 test PC board replaces the discretes and antenna of the RF access point.

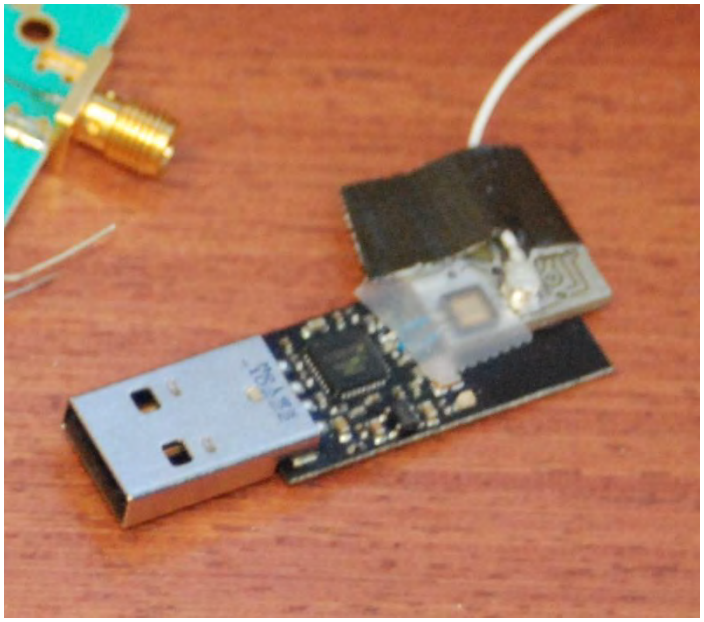

Figure 5. Photo of the ARL29 test PC board attached to the RF access point.

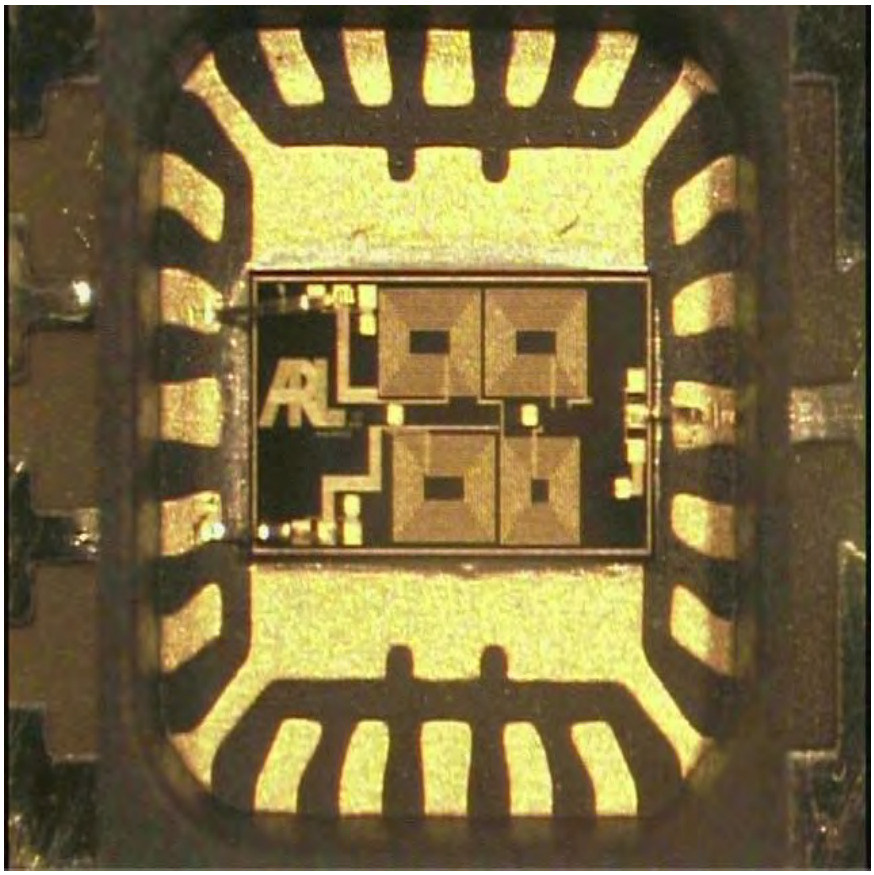

Figure 6. Photo of the ARL29M425 IC wirebonded in a 4x4 mm QFN package.

The top portion of the PC board has the ARL29M425S IC (U2) in a 4x4 mm QFN package with its two RF connections as small UFL RF connectors (J6, J7). Again, to test the matching circuit ICs, the discrete matching components L2, L3, C16, and C17 plus the chip antenna are removed (figure 7). The test board is attached to the RF access point board and short wire connections are made to the two RF connections of the CC1111 RFIC (L3, C17 pads). Figure 8 shows a photo of the actual assembled test board and RF access point PC board. The jumpers are set to select J7 as ―on‖ but swapping the jumpers will enable the connection to J6. A supply voltage of about ―2.5 V" is needed to drive the pseudomorphic high electron mobility transistor (PHEMT) switches. Figure 9 shows the wire bonding of the 50x95 mil ARL29M425S die in a 4x4 mm QFN package.

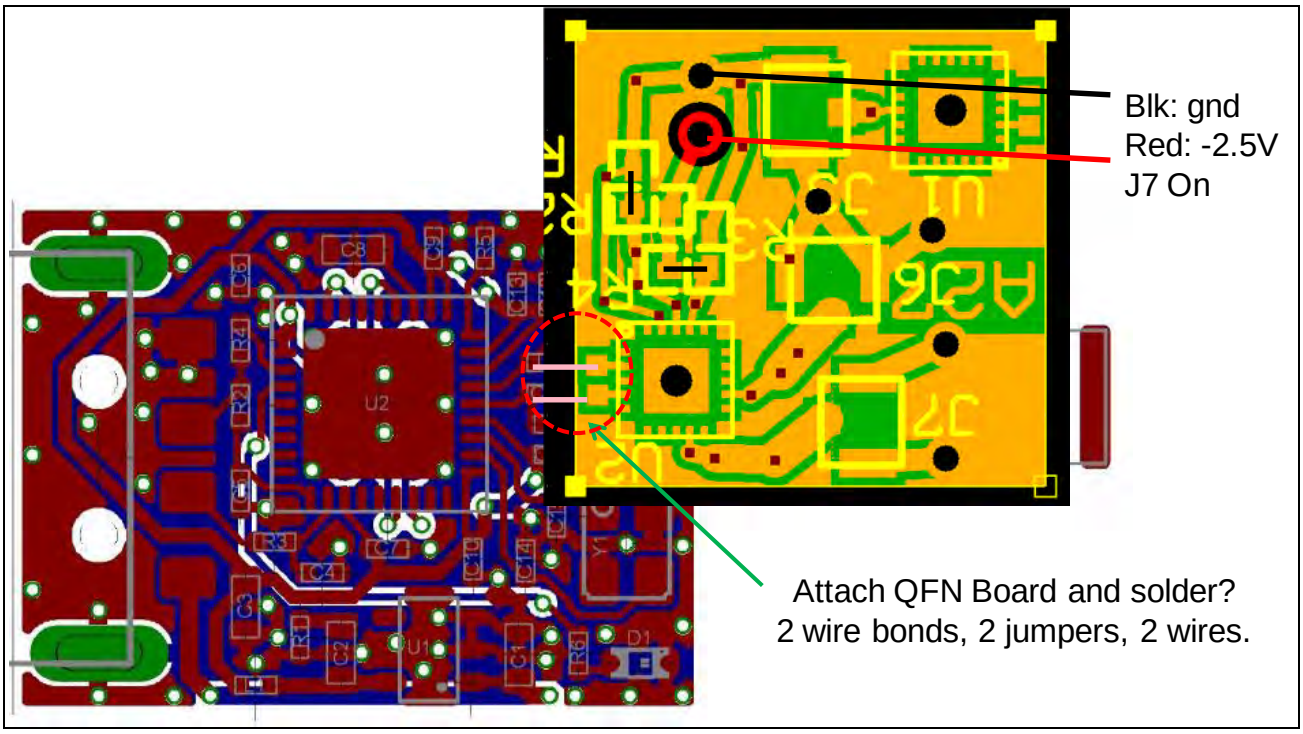

Figure 7. ARL29M425S test PC board replaces the discretes and antenna of the RF access point.

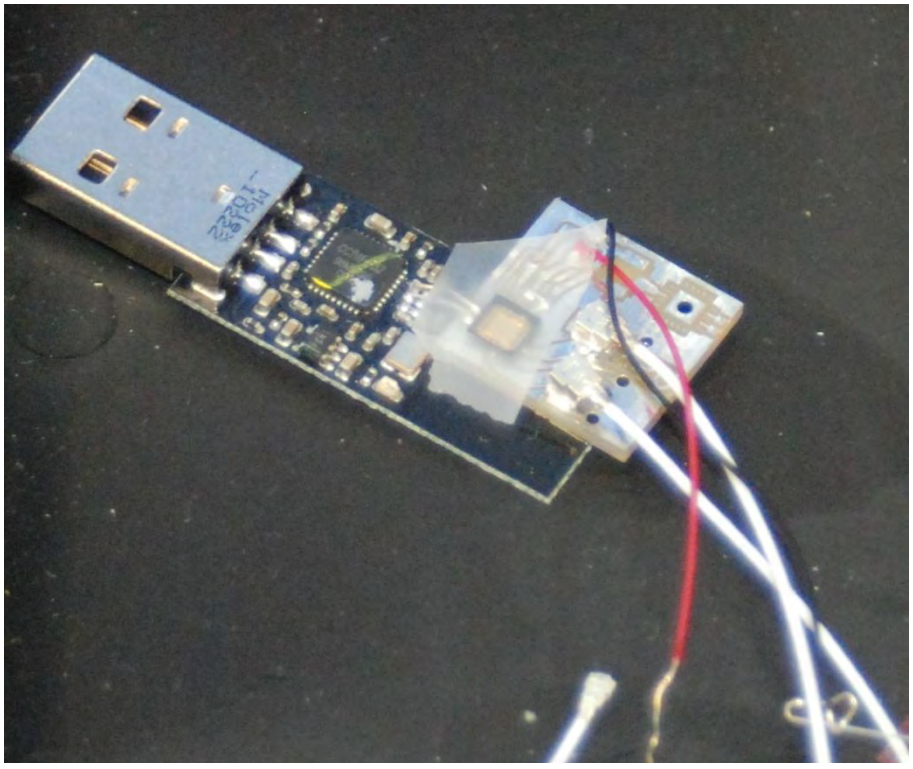

Figure 8. Photo of the ARL29M425S test PC board attached to the RF access point.

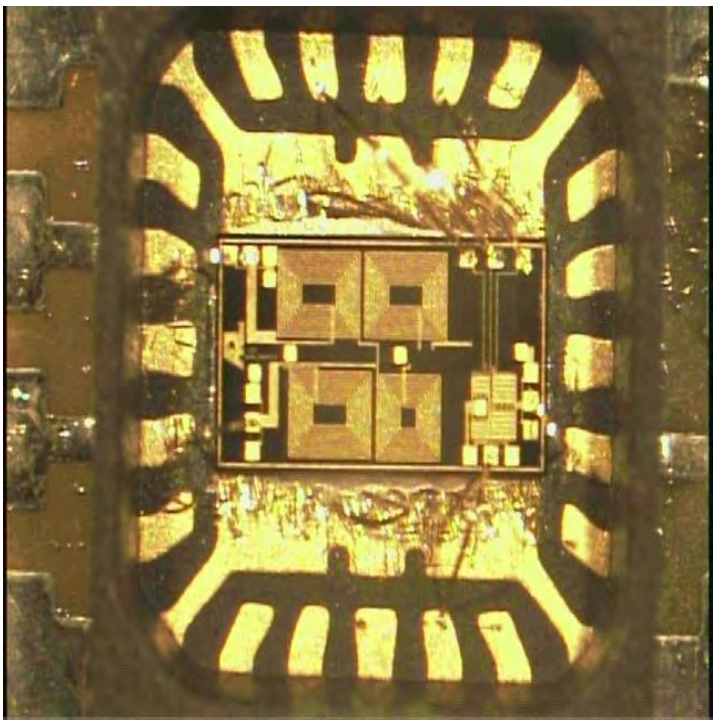

Figure 9. Photo of the ARL29M425S IC wirebonded in a 4x4 mm QFN package.

5. Testing of the 433-MHz Matching IC (ARL29M425)

An Agilent N1912A P-series power meter was used to measure the power level transmitted using the RF access point during transmit pulses with the Chronos development kit software. The computer is set up to emulate a heart rate monitor transmitting heart rates from 40 bps, incrementing continuously with updates every second. First, a 433-MHz RF access point board was modified, as shown in figure 10, removing the chip antenna and replacing it with a small UFL RF connector. This could then be connected via cables and adapters to measure the RF output of the base RF access point board versus the previously modified boards, which use the Booster IC matching designs to replace the many discrete components (figures 5 and 8). It should be noted that the chip antenna for the 433-MHz board has an 868-MHz part number and is much smaller than the chip antenna designed for 433-MHz operation fabricated by the same manufacturer, Johanson. Possibly, the smaller 868-MHz chip antenna is used at some resonance that is not efficient but works reasonably well at the lower 433-MHz frequency. The datasheet for the 868-MHz part does not give a matching circuit or any information on using it at 433 MHz. It should also be noted that the Booster IC matching circuits were designed for a 50-ohm system. For the RF access point board, it appears that a couple of the discrete matching elements are used to match the chip antenna, which is not a 50-ohm match. This may explain

why the power levels of the modified RF access point board (figure 10) are much lower than the matched designs.

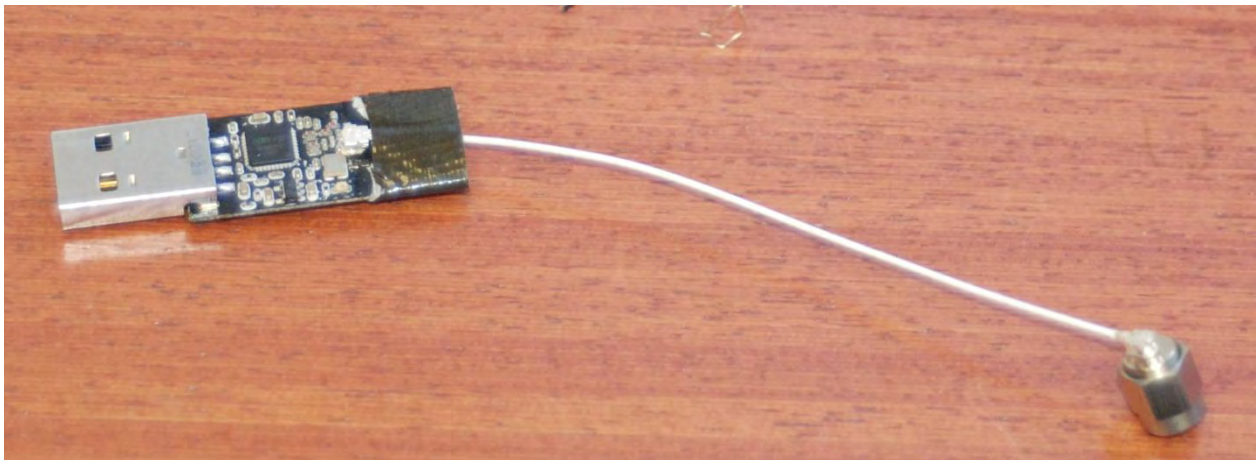

Figure 10. RF access point board with a UFL connector replacing the chip antenna.

The measured power levels transmitted with the heart rate monitor test are consistent relative to each other, but presets on the Agilent N1912A power meter were used for GSM and Bluetooth mode settings without clearly understanding why the absolute power levels differed by about 0.8 dB between these two ~~–~~easy to use" presets. Obviously, the heart rate monitor test pulse is neither a GSM nor Bluetooth compatible pulse, but these two presets made for consistent measurements for these tests (see table 1).

Table 1. Measured power levels of modified 433-MHz RF access point boards.

N1912A Mode Setting	ARL29M425 (figure 6)	RF Access Point (figure 10)
Peak	7.46 dBm	–1.92 dBm
Bluetooth	6.70 dBm	–2.73 dBm
GSM	5.89 dBm	–3.41 dBm

The switched matching circuit ARLM425S was originally measured with similar power levels at one of the RF connectors (J6)—7.00, 6.89, and 6.19 dBm for the three mode settings on the power meter—but then seemed to quit working. There was only one board made using this part and since it appeared to operate similar to the non-switched part, as expected, no further debugging was performed to this board. Matching circuits can be custom integrated into the Booster IC if desired and could be designed for broadband or dual-band operation for a given COTS RFIC transceiver.

Figure 11 shows measured return loss for the RF access point with the chip antenna removed (magenta), with the matching circuit ARL29M425 (blue), and for a typical 433-MHz chip antenna with the proper discrete matching components (red). It seems to verify that removing the chip antenna and connecting directly to a 50-ohm UFL connector results in a poor match and may explain the low power levels measured with the RF access board (figure 10, table 1). The

integrated matching circuit of ARL29M425 (figure 6) provides better return loss with room for further optimization/customization, if desired, in future designs. The good return loss shown in the figure is for a matched 433-MHz chip antenna; however, the RF access board is using an unknown match to a smaller 868-MHz chip antenna.

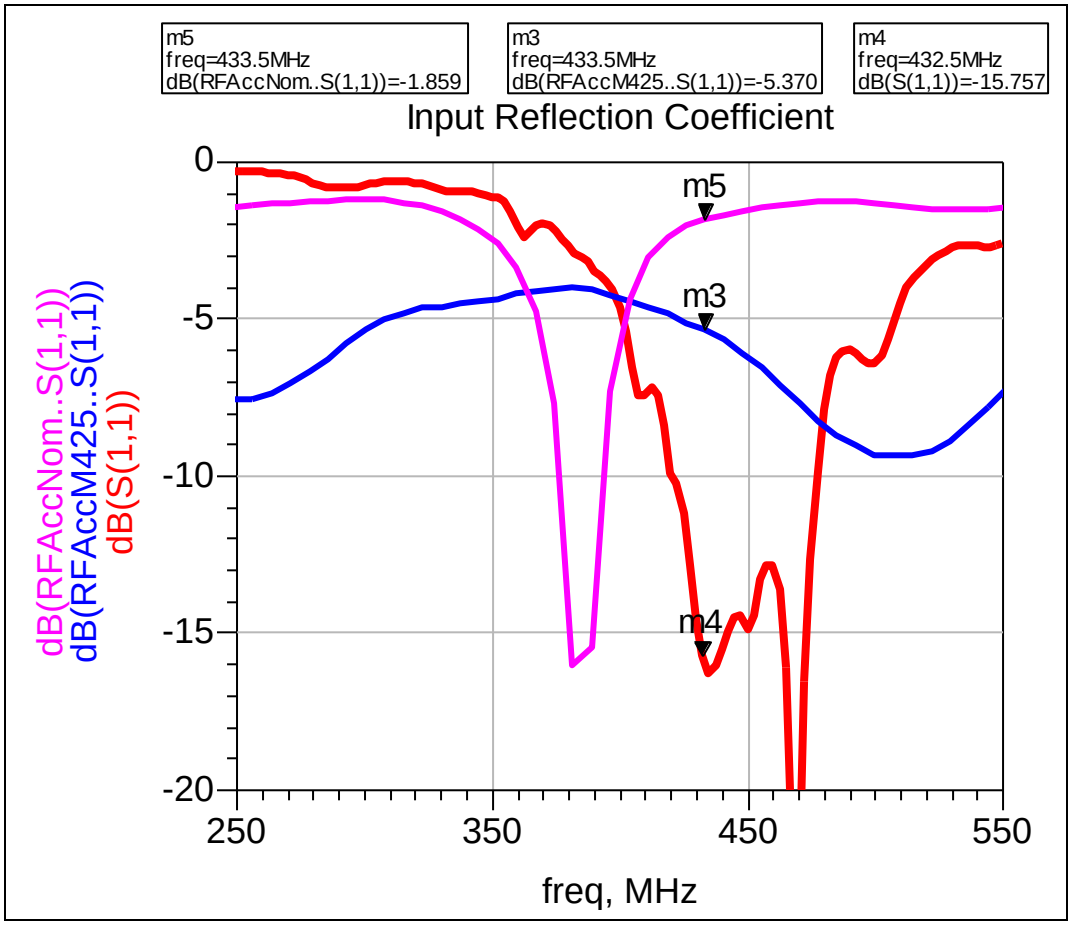

Figure 11. Measured RF return loss of the access point with and without matching.

The test of the 433-MHz integrated passive matching circuit Booster IC demonstrates that the many discrete lumped elements components required for matching a typical COTS RFIC can be replaced by a custom part. It also illustrates that it is important to customize the design for the particular RFIC and the system. The passive Booster IC was designed to 50 ohms but could have been designed to absorb the few lumped element matching elements required by the chip antenna, in case a non-50-ohm antenna is used for the system. Each COTS RFIC typically pushes these many discrete matching elements outside of the Si IC package onto the system PC board. In order to broadband the system, one would need to also broadband the matching elements for the desired COTS RFIC. The tradeoff is SWAP versus cost, and complexity as to what should be optimally integrated for each system. This is partly why the Booster ICs for the 2nd pass were divided into passive matching elements versus the active RF front end portion. The active portions could have a consistent architecture for use with various COTS RFICs and

the passive portions could be optimized to a particular COTS RFIC and frequency band, or bands. Next, an example of a dual-band matching IC was tested.

6. Simple PC Board to Test the 433/915-MHz Dual-band Matching IC (ARL26DB)

A simple PC board was created to test the ARL26DB Booster IC, which contains switches to connect the single antenna connection to an RF input and output connection for direct use with the active Booster IC designs and their separate single-ended RF connections for transmit and receive. It also contains switches to choose between a matching circuit designed for 433-MHz band operation and another matching circuit for 915-MHz operation. While the CC11XX RFIC can operate at either of these bands, the typical system application uses discrete matching components, which restrict the system use to a single narrowband choice. Figure 12 shows the simple schematic of the board design using ExpressPCB software.

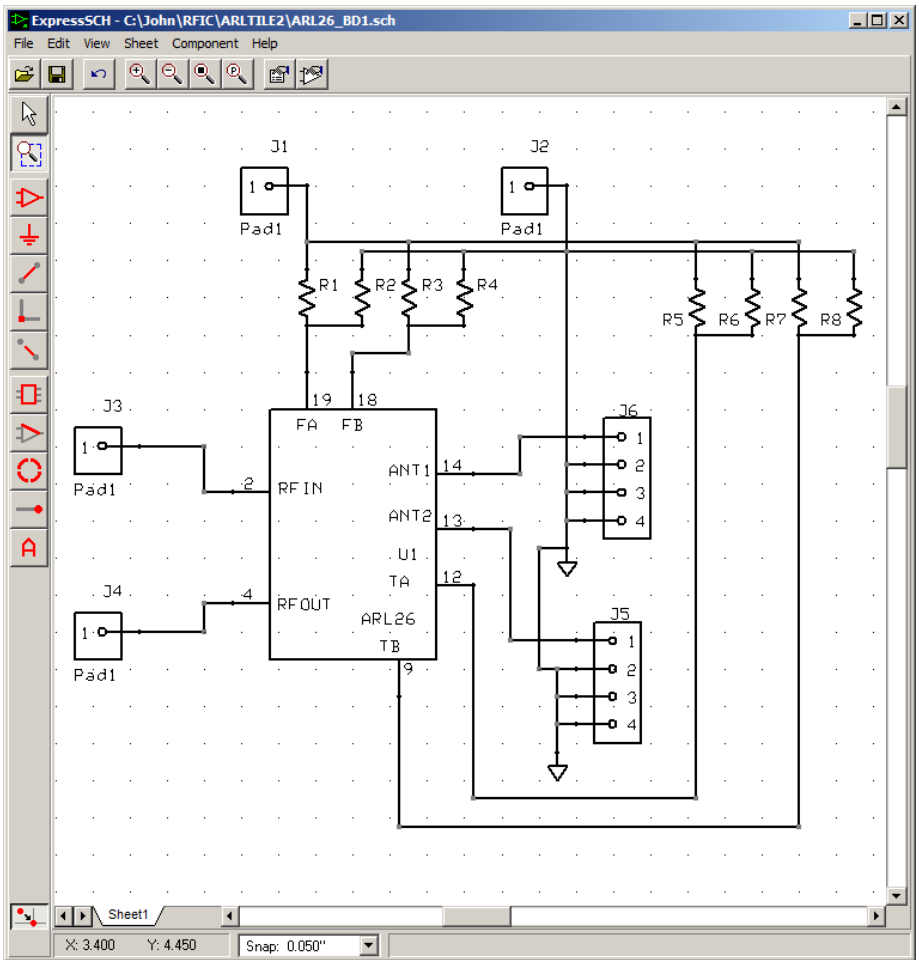

Figure 12. Schematic of the ARL26DB integrated matching RF circuit test PC board.

The schematic shows the dual RF differential connections to the CC11XX RFIC on the left and two RF connections for the ARL26DB matching circuit (J5, J6) on the right. Jumper wires or resistors are used to configure the test PC board for the frequency band (433 or 915 MHz), and for the RF function (transmit or receive). Figure 13 shows the simple two-sided board layout of the test board, which overlays the RF access point board to replace its discrete matching components. The bottom left board component U1 is the ARL26DB Booster IC packaged in a 4x4 mm QFN package. Two RF connections for the transmit and receive paths of the ARL29M425S matching circuit (J5, J6) are located in the middle, and eight jumpers or resistors (R1–R8) are along the top for configuring the frequency band and direction of the RF (transmit/receive).

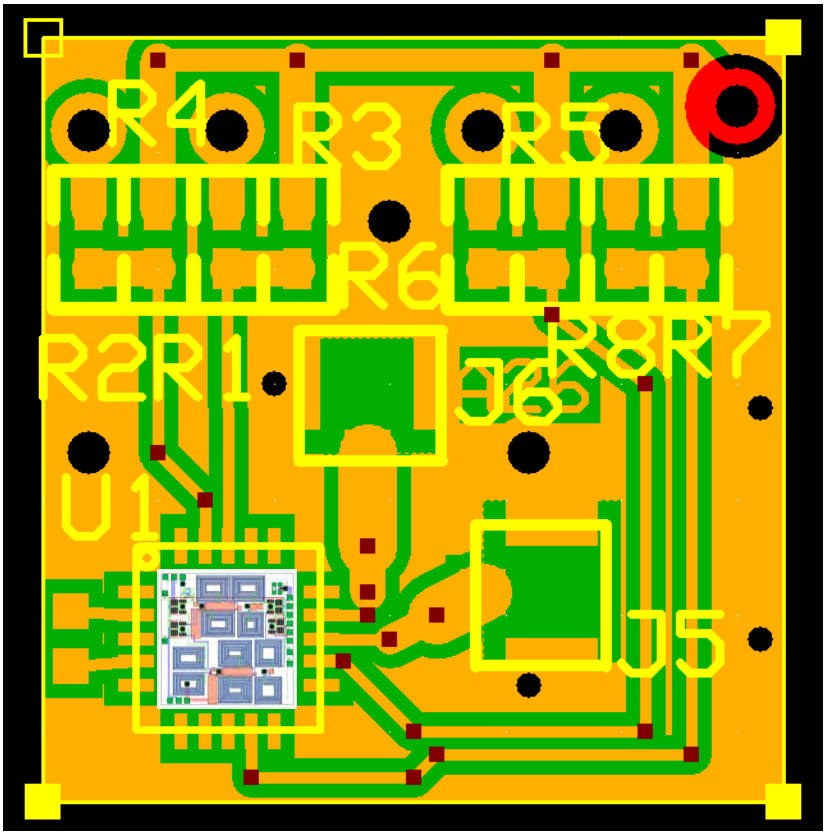

Figure 13. Layout of the ARL26DB integrated matching RF circuit test PC board.

To test the matching circuit IC, the discrete matching balun U3 plus the chip antenna are removed (figure 14). The test board is attached to the RF access point board and short wire connections are made to the two RF connections of the CC1111 RFIC (U3 pads). Since the matching circuits within the dual-band design contain the same 433-MHz matching topology tested in the fixed-band ARL29M425 IC, the dual-band design was only tested in the higher 915-MHz configuration. This required a modification of the fixed 915-MHz RF access point design. This required no change to the preprogrammed CC1111 RFIC transceiver as it was already configured for 915-MHz operation. Another caveat of the testing, however, was that the

ARL26DB design was intended as a demonstration of a dual-band matching capability. Its enhancement mode (E-mode) PHEMT switches only require 0 and +0.8 V for configuration. This presented a small problem in the test as the power levels of the CC1111 should be reduced from its full power levels (<10 dBm), which exceed the 0.8-V threshold of the switches, originally only intended for small signal operation. Thus, the output pulses of the test exceeded small signal operation and were reduced, or attenuated, to a lower power level. The test results do demonstrate that the switched matching circuit could be used for both bands but either the power level of the RFIC should be configured for small-signal operation, or the custom matching circuit should use depletion mode (D-mode) PHEMT devices for switching to avoid the attenuation of the RF signal. Figure 15 shows a photo of the actual assembled test board and RF access point PC board.

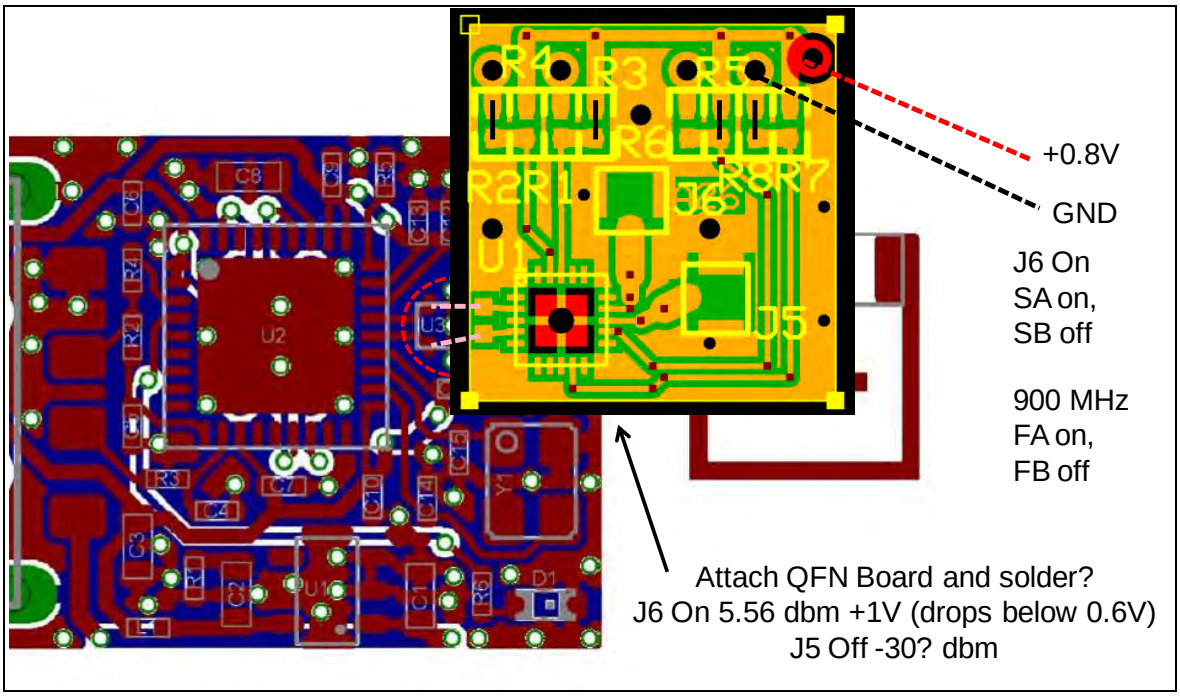

Figure 14. ARL26DB test PC board replaces the discretes and antenna of RF access point.

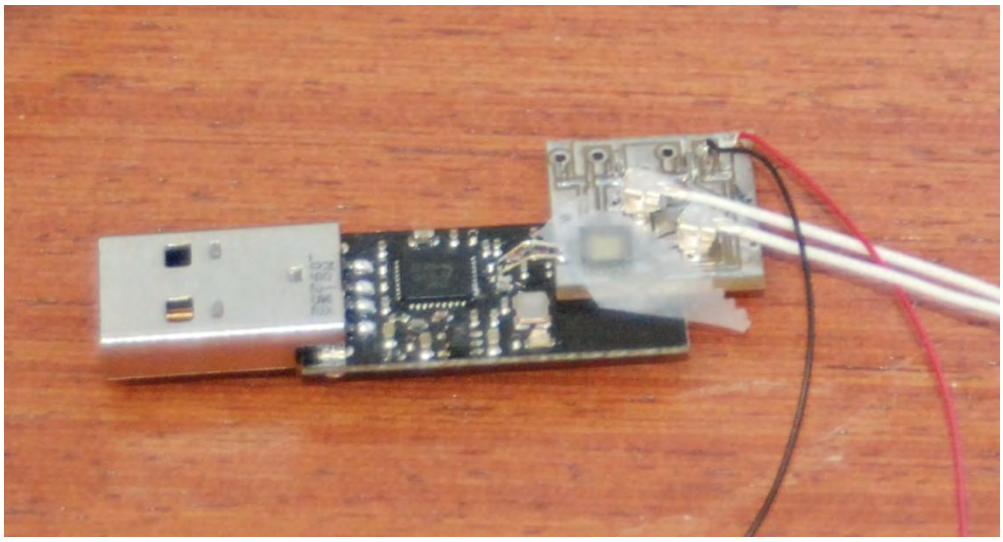

Figure 15. Photo of the ARL26DB test PC board attached to the RF access point.

7. Testing of the 433/915-MHz Dual-band Matching IC (ARL26DB)

An Agilent N1912A P-series power meter was used to measure the power level transmitted using the RF access point during transmit pulses with the Chronos development kit software. The computer is set up to emulate a heart rate monitor transmitting heart rates with updates every second. First, a 915-MHz RF access point board was modified, as shown in figure 15, removing the chip antenna and balun and replacing it with the dual-band ARL26 test board. This could then be connected via cables and adapters to measure the output of the RF access point board plus the passive Booster IC replacing the many discrete matching components.

The measured power levels of the 915-MHz RF access point PC board were several dB lower than the 433-MHz version due to the attenuation of the E-mode switches used in the ARL26DB Booster IC, which was only designed for small signal operation. However, it did successfully demonstrate the concept of having switched band matching circuits. In spite of the large signal clipping, the Chronos watch successfully received the transmitted heart rate pulses at 915 MHz.

8. PC Board to Simplify Testing with the Active Booster ICs (ARL21-24)

A simple PC board was created to simplify RF testing with the Active Booster ICs. Previously, these parts were tested in QFN packages on boards with SMA connectors, but a new version of the PC board was fabricated to simplify testing. The newer boards will be especially useful for testing with the system integrator's tag, which has breakout RF test points. For the 2nd pass active designs, all of the four active variations have the same overall topology and footprint.

Figure 16 shows the typical wire bonding in the 4x4 mm QFN package. The control inputs for the transmit/receive switch are TA, TB = 2.8 V, 0 V for the receive path (low-noise amplifier [LNA]); and TA, TB = 0 V, 2.8 V for the transmit path (power amplifier [PA]). When in transmit mode, the control inputs for the binary phase shift keying (BPSK) modulator are VA, VB = 2.8 V, 0 V for the low pass (LP) state; and VA, VB = 0 V, 2.8 V for the high pass (HP) state.

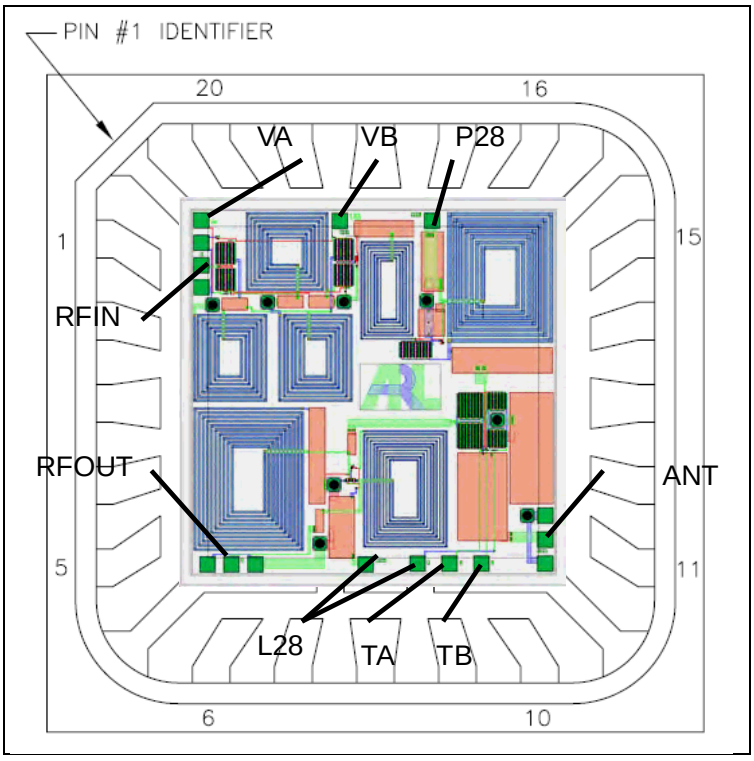

Figure 16. Wirebond diagram for booster ICs (ARL21-24) in 4x4 mm QFN package.

Figure 17 shows the simple schematic of the board design using ExpressPCB software. The board has 3 RF SMA connectors for RF input (receive), RF output (transmit), and antenna, plus two 4-pin connectors for power and control signals. The four control signals can be driven externally or can use dual inline package (DIP) switches and pullup resistors on the PC board to simplify testing of the various modes (transmit/receive, and high-pass/low-pass BPSK). Figure 18 shows the layout of the PC board design using ExpressPCB software.

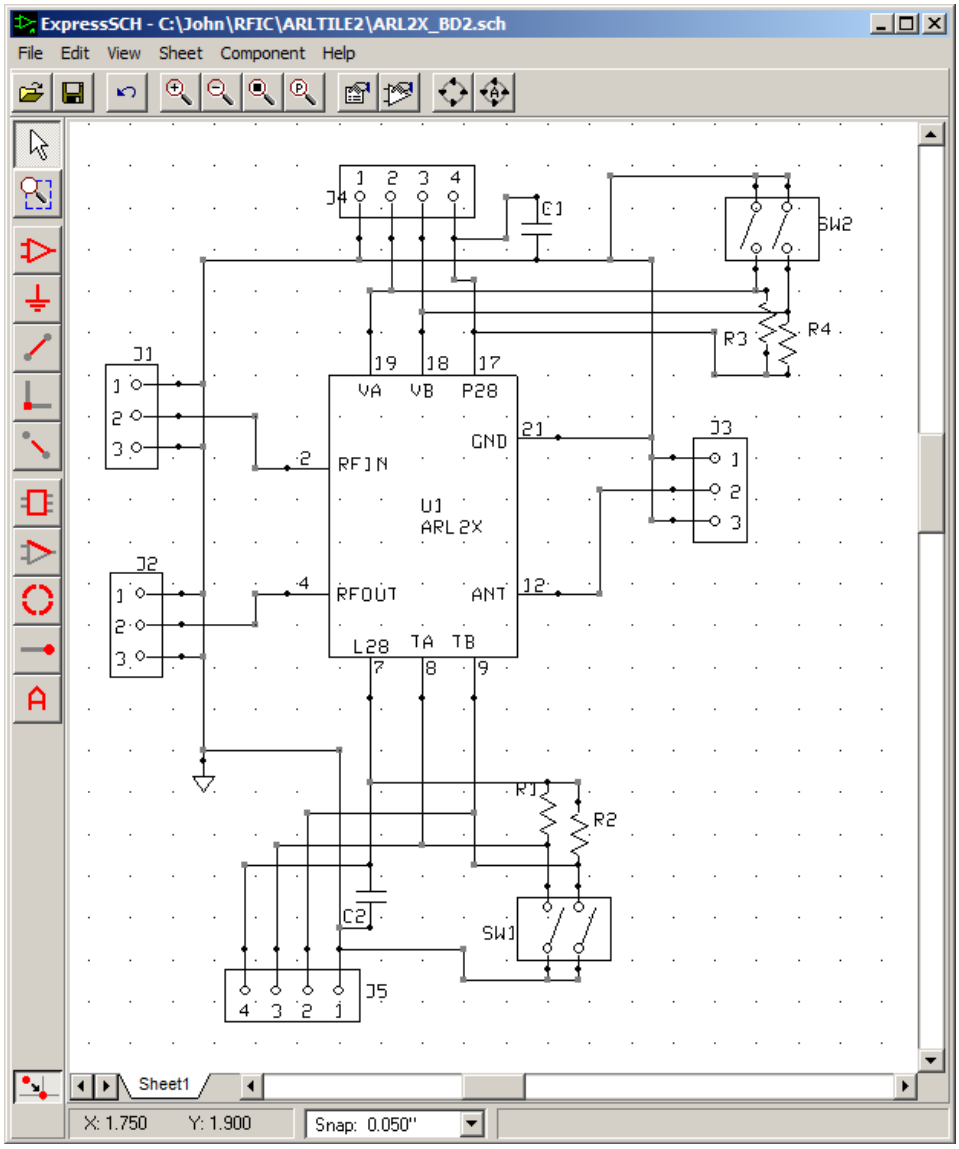

Figure 17. Schematic of the ARL2X active booster IC test PC board.

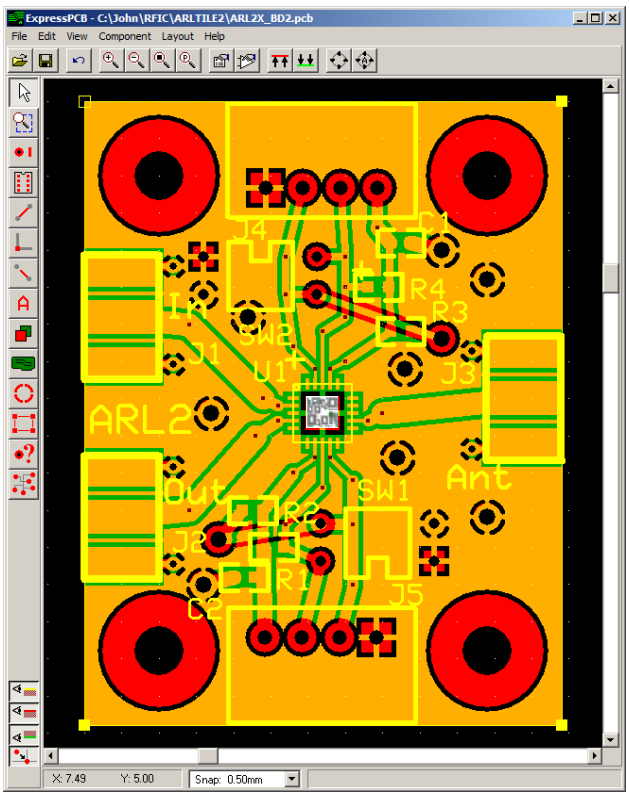

Figure 18. Layout of the ARL2X active booster IC test PC board.

9. Testing Results for the Active Booster ICs (ARL21-24)

The simple PC board described previously was used to create a test board populated with a QFN packaged version of each of the four 2nd pass Active Booster ICs. Results should compare to those measured previously at the bare die probe level as well as previous QFN package tests. Following are the results for the four Active Booster Designs, which will be used for testing with the RF access point system to illustrate the performance enhancements possible when combined with a COTS wireless RF system:

- ARL21M425—This 425-MHz design contains a BPSK modulator, a 100-mW PA for 2.8 V, a narrowband low DC power consumption LNA, and a transmit/receive (TR) switch using positive voltage control inputs with negative threshold depletion PHEMTs.

Figure 19 shows the measured S-parameter performance of the test board with ARL21M425 at 2.8 V in the two transmit states of the BPSK modulator. Power performance of the design at 2.8 and 3.3 V is shown in tables 2 and 3 along with a plot of this data in figure 20. Figure 21 shows the measured S-parameter performance of the test board with ARL21M425 at 2.8 V in the receive state along with a summary of the LNA's noise figure and gain in table 4.

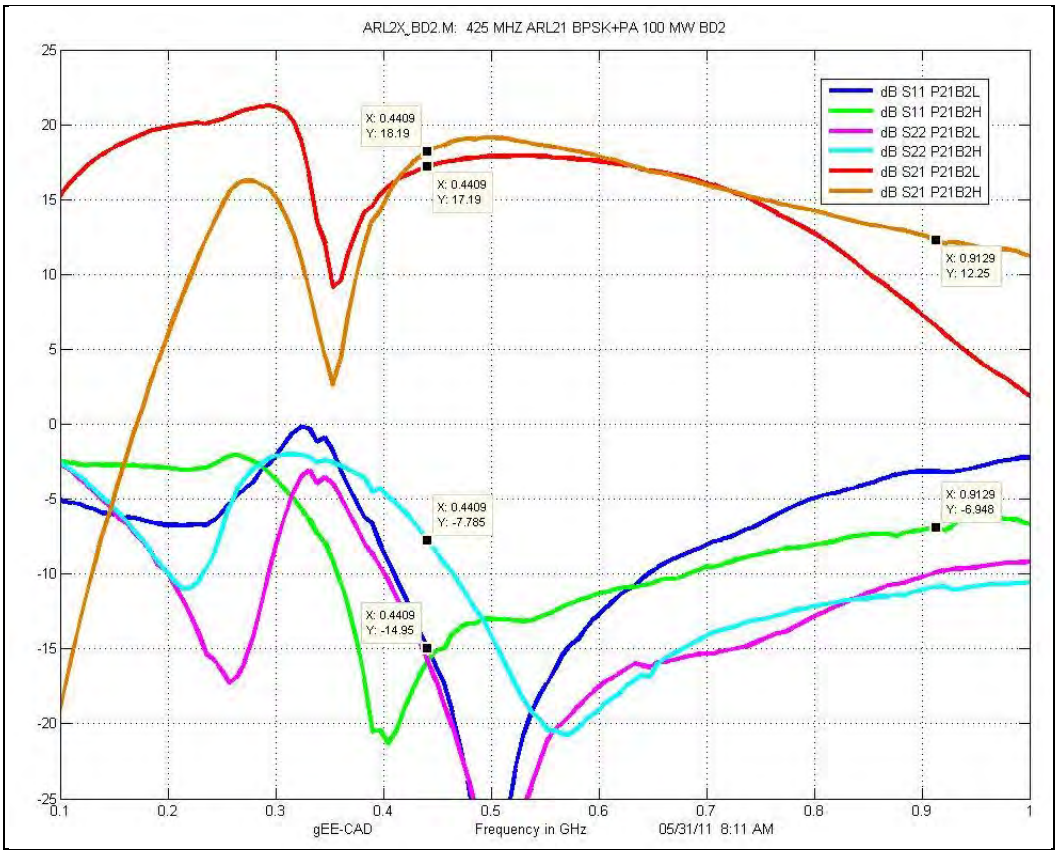

Figure 19. Measured S-parameters of the ARL21M425 transmit states (2.8 V 84 mA).

Table 2. Measured power performance of ARL21M425 at 2.8 V.

0.35 dB offset at input for 433 MHz				Includes LNA current			
ARL21 ARLTILE2 TQPED				2.8V ; 84 mA			
Pin(corr)	**Pout(corr)**	**Gain**	**I1(2.8V)**	**PDC(mw)**	**Pout(mw)**	**Drn Eff**	**PAE**
-15.35	2.80	18.15	84	235.2	1.91	0.8	0.8
-10.35	7.74	18.09	84	235.2	5.94	2.5	2.5
-8.35	9.76	18.11	83	232.4	9.46	4.1	4.0
-6.35	11.71	18.06	83	232.4	14.83	6.4	6.3
-4.35	13.61	17.96	83	232.4	22.96	9.9	9.7
-2.35	15.40	17.75	82	229.6	34.67	15.1	14.8
-1.35	16.17	17.52	82	229.6	41.40	18.0	17.7
-0.35	16.82	17.17	82	229.6	48.08	20.9	20.5
0.65	17.33	16.68	83	232.4	54.08	23.3	22.8
1.65	17.73	16.08	83	232.4	59.29	25.5	24.9
2.65	18.06	15.41	83	232.4	63.97	27.5	26.7
3.65	18.33	14.68	83	232.4	68.08	29.3	28.3

Table 3. Measured power performance of ARL21M425 at 3.3 V.

433 MHz	Package E	ARL21 ARLTILE2 TQPED				3.3V ; 87 mA			
Pin(SG)	**Pout(PM)**	**Pin(corr)**	**Pout(corr)**	**Gain**	**I1(3.3V)**	**PDC(mw)**	**Pout(mw)**	**Drn Eff**	**PAE**
-15.0	2.66	-15.35	2.66	18.01	87	287.1	1.85	0.6	0.6
-10.0	7.62	-10.35	7.62	17.97	86	283.8	5.78	2.0	2.0
-8.0	9.66	-8.35	9.66	18.01	86	283.8	9.25	3.3	3.2
-6.0	11.61	-6.35	11.61	17.96	86	283.8	14.49	5.1	5.0
-4.0	13.53	-4.35	13.53	17.88	85	280.5	22.54	8.0	7.9
-2.0	15.36	-2.35	15.36	17.71	85	280.5	34.36	12.2	12.0
-1.0	16.22	-1.35	16.22	17.57	85	280.5	41.88	14.9	14.7
0.0	16.99	-0.35	16.99	17.34	86	283.8	50.00	17.6	17.3
1.0	17.64	0.65	17.64	16.99	87	287.1	58.08	20.2	19.8
2.0	18.18	1.65	18.18	16.53	89	293.7	65.77	22.4	21.9
3.0	18.62	2.65	18.62	15.97	90	297.0	72.78	24.5	23.9
4.0	19.00	3.65	19.00	15.35	90	297.0	79.43	26.7	26.0
5.0	19.28	4.65	19.28	14.63	90	297.0	84.72	28.5	27.5

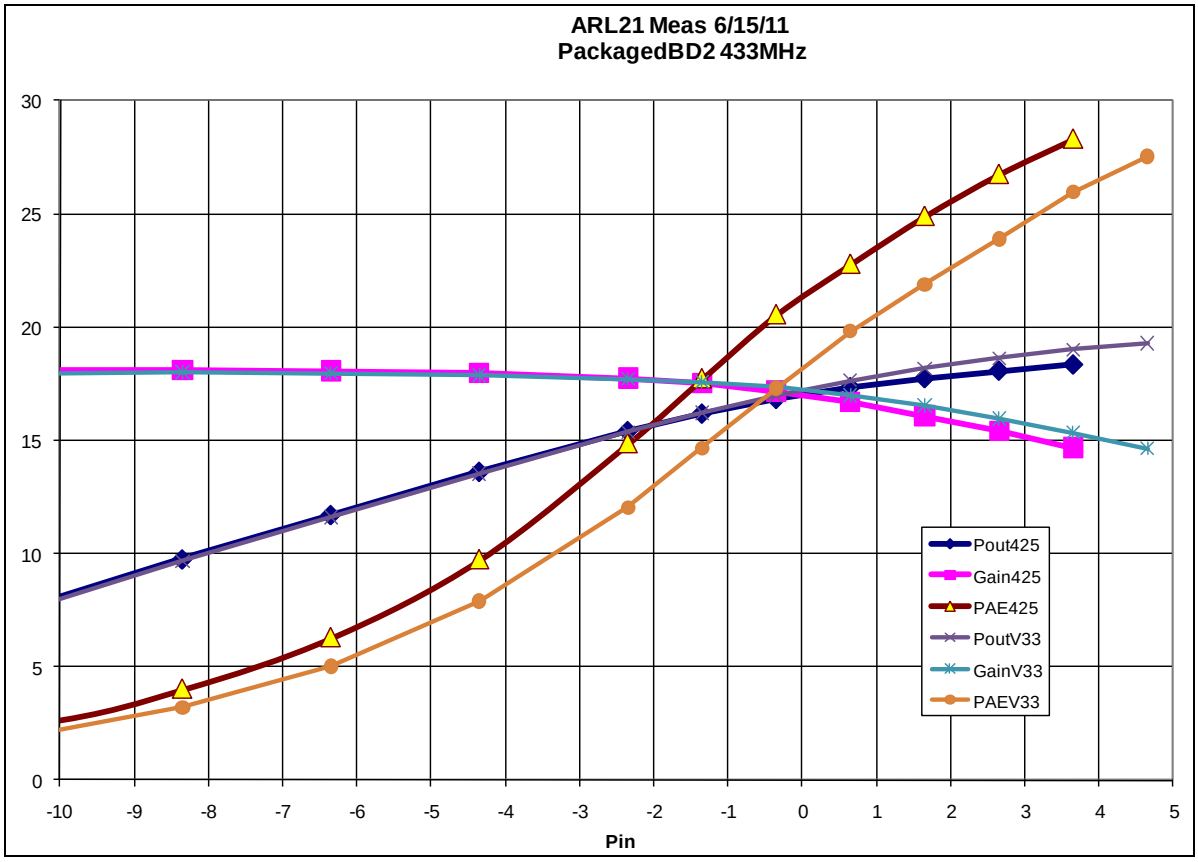

Figure 20. Plot of the gain, output power, and power-added efficiency (PAE) of the ARL21M425 at 2.8 and 3.3 V.

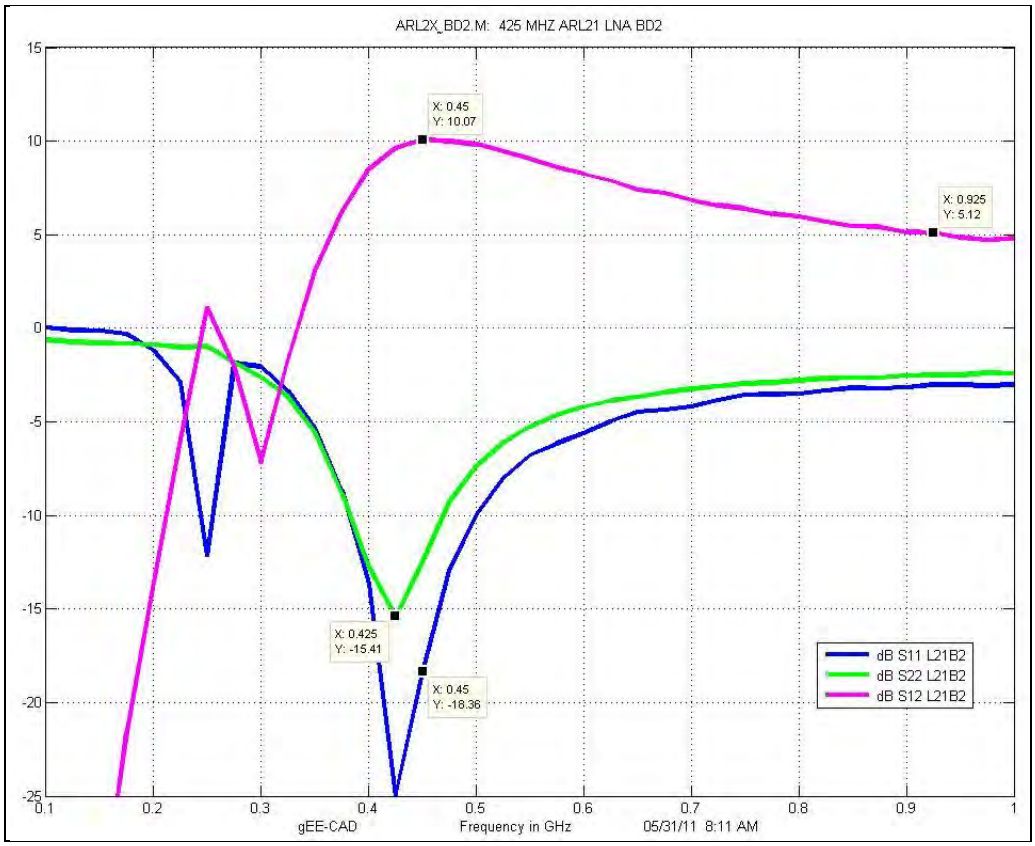

Figure 21. Measured S-parameters of the ARL21M425 receive state (2.8 V, 84 mA).

Table 4. Measured noise figure and gain of the ARL21M425 (2.8 V).

LNA		
Freq(MHz)	Gain	NF
400.0	8.56	3.60
450.0	10.61	5.01
500.0	9.98	5.05
550.0	9.30	4.69
600.0	8.73	4.33
650.0	7.52	3.67

- ARL22M425—This 425-MHz design contains a BPSK modulator, a 50-mW PA for 2.8 V, a narrowband low DC power consumption LNA, and a TR switch using positive voltage control inputs with negative threshold depletion PHEMTs.

Figure 22 shows the measured S-parameter performance of the test board with ARL23M425 at 2.8 V in the two transmit states of the BPSK modulator. Power performance of the design at 2.8 and 3.3 V is shown in tables 5 and 6 along with a plot of this data in figure 23. Figure 24 shows the measured S-parameter performance of the test board with ARL22M425 at 2.8 V in the receive state along with a summary of the LNA's noise figure and gain in table 7.

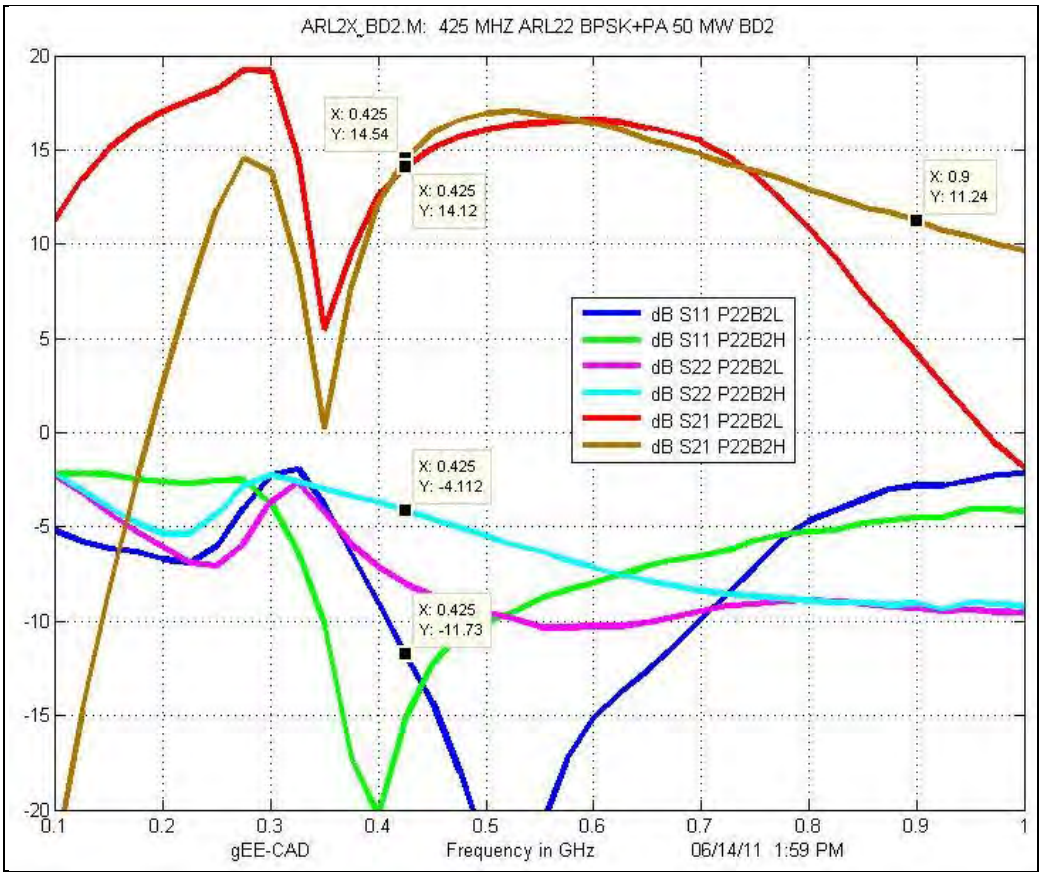

Figure 22. Measured S-parameters of the ARL22M425 transmit states (2.8 V, 45 mA).

Table 5. Measured power performance of ARL22M425 at 2.8 V.

0.35 dB offset at input for 433 MHz				Includes LNA current			
ARL22 ARLTILE2 TQPED				2.8V ; 45 mA			
Pin(corr)	**Pout(corr)**	**Gain**	**I1(2.8V)**	**PDC(mw)**	**Pout(mw)**	**Drn Eff**	**PAE**
-15.35	-0.19	15.16	45	126.0	0.96	0.8	0.7
-10.35	4.73	15.08	45	126.0	2.97	2.4	2.3
-8.35	6.76	15.11	46	128.8	4.74	3.7	3.6
-6.35	8.66	15.01	46	128.8	7.35	5.7	5.5
-4.35	10.48	14.83	47	131.6	11.17	8.5	8.2
-2.35	12.21	14.56	49	137.2	16.63	12.1	11.7
-1.35	13.00	14.35	50	140.0	19.95	14.3	13.7
-0.35	13.75	14.10	52	145.6	23.71	16.3	15.7
0.65	14.42	13.77	54	151.2	27.67	18.3	17.5
1.65	15.02	13.37	55	154.0	31.77	20.6	19.7
2.65	15.53	12.88	57	159.6	35.73	22.4	21.2
3.65	15.95	12.30	57	159.6	39.36	24.7	23.2

Table 6. Measured power performance of ARL22M425 at 3.3 V.

433 MHz	Package E	ARL22 ARLTILE2 TQPED				3.3V ; 47 mA			
Pin(SG)	**Pout(PM)**	**Pin(corr)**	**Pout(corr)**	**Gain**	**I1(3.3V)**	**PDC(mw)**	**Pout(mw)**	**Drn Eff**	**PAE**
-15.0	-0.28	-15.35	-0.28	15.07	47	155.1	0.94	0.6	0.6
-10.0	4.65	-10.35	4.65	15.00	47	155.1	2.92	1.9	1.8
-8.0	6.68	-8.35	6.68	15.03	47	155.1	4.66	3.0	2.9
-6.0	8.58	-6.35	8.58	14.93	48	158.4	7.21	4.6	4.4
-4.0	10.42	-4.35	10.42	14.77	49	161.7	11.02	6.8	6.6
-2.0	12.15	-2.35	12.15	14.50	50	165.0	16.41	9.9	9.6
-1.0	12.92	-1.35	12.92	14.27	51	168.3	19.59	11.6	11.2
0.0	13.64	-0.35	13.64	13.99	53	174.9	23.12	13.2	12.7
1.0	14.31	0.65	14.31	13.66	54	178.2	26.98	15.1	14.5
2.0	14.93	1.65	14.93	13.28	56	184.8	31.12	16.8	16.0
3.0	15.49	2.65	15.49	12.84	57	188.1	35.40	18.8	17.8
4.0	15.98	3.65	15.98	12.33	59	194.7	39.63	20.4	19.2
5.0	16.41	4.65	16.41	11.76	60	198.0	43.75	22.1	20.6

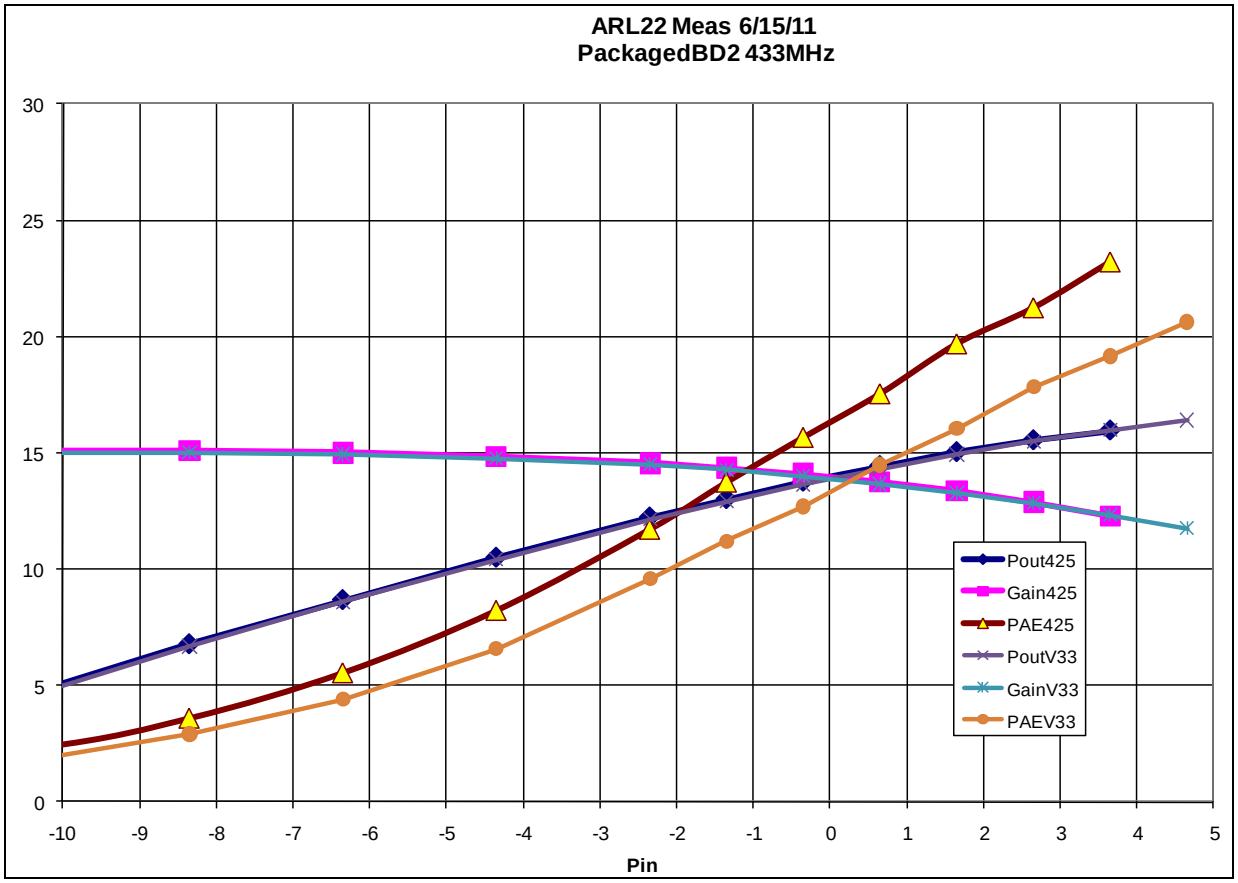

Figure 23. Plot of the gain, output power, and PAE of ARL22M425 at 2.8 and 3.3 V.

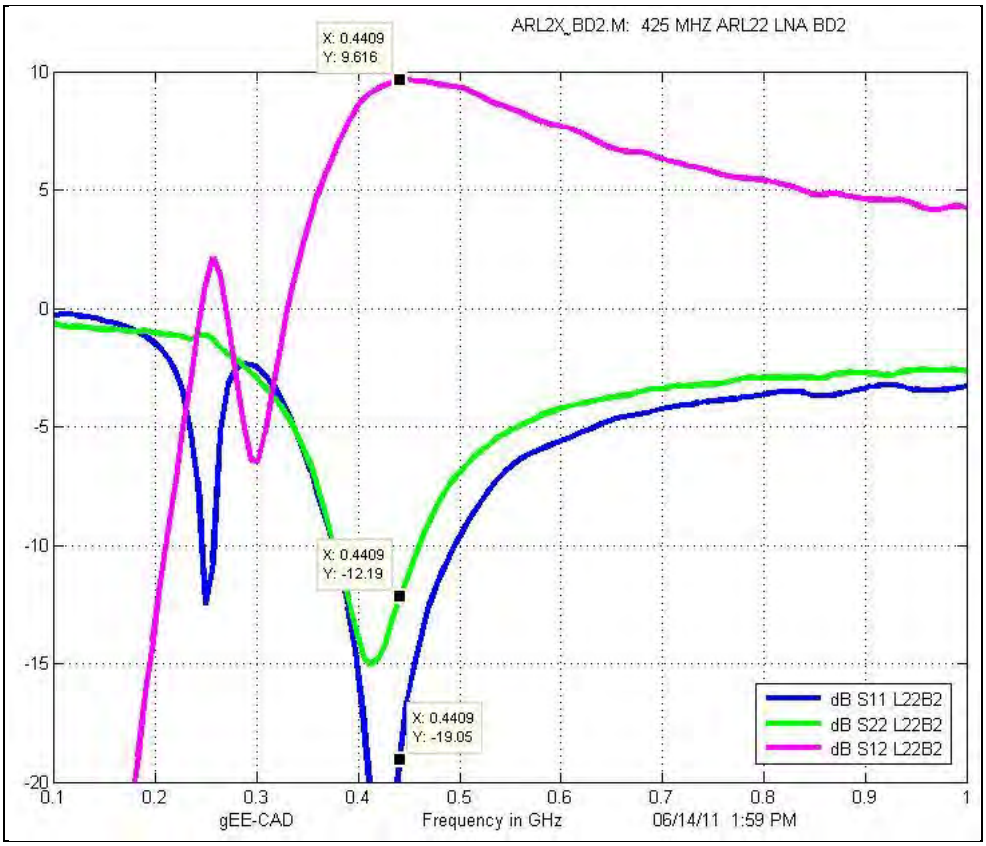

Figure 24. Measured S-parameters of the ARL22M425 receive state (2.8 V, 45 mA).

Table 7. Measured noise figure and gain of ARL22M425 (2.8 V).

LNA		
Freq(MHz	Gain	NF
400.0	8.92	4.07
450.0	10.47	5.10
500.0	9.63	4.96
550.0	8.97	4.58
600.0	8.46	4.26
650.0	7.27	3.58

- ARL23M425—This 425-MHz design contains a BPSK modulator, a 50/75-mW PA for 2.8/3.6 V, a narrowband low DC power consumption LNA, and a TR switch using positive voltage control inputs with negative threshold depletion PHEMTs. This design is intended to operate over a broad range of battery voltages.

Figure 25 shows the measured S-parameter performance of the test board with ARL23M425 at 2.8 V in the two transmit states of the BPSK modulator. Power performance of the design at 2.8 and 3.3 V is shown in tables 8 and 9 along with a plot of this data in figure 26. Figure 27 shows

the measured s-parameter performance of the test board with ARL23M425 at 2.8 V in the receive state along with a summary of the LNA's noise figure and gain in table 10.

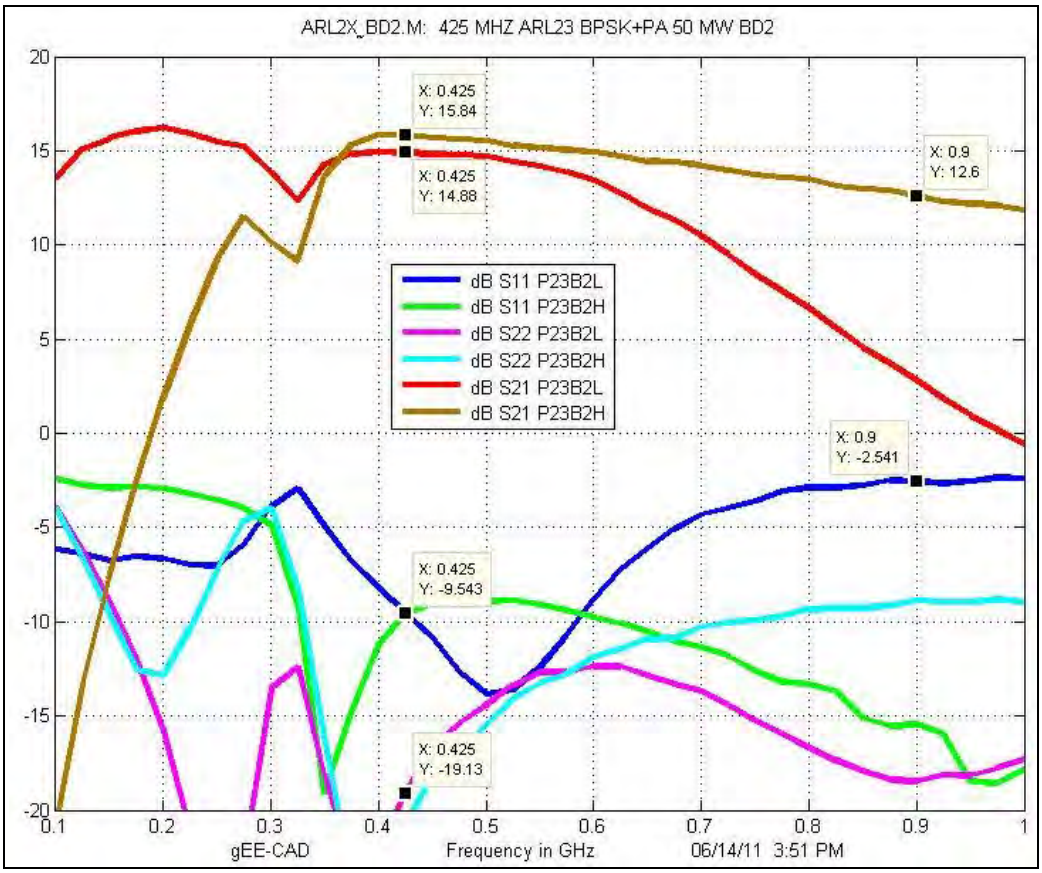

Figure 25. Measured S-parameters of the ARL23M425 transmit states (2.8 V, 51 mA).

Table 8. Measured power performance of ARL23M425 at 2.8 V.

Uses BB LNA from ARLTILE1							
0.35 dB offset at input for 433 MHz				Includes LNA current			
ARL23 ARLTILE2 TQPED				2.8V ; 51 mA			
Pin(corr)	**Pout(corr)**	**Gain**	**I1(2.8V)**	**PDC(mw)**	**Pout(mw)**	**Drn Eff**	**PAE**
-15.35	0.59	15.94	51	142.8	1.15	0.8	0.8
-10.35	5.56	15.91	51	142.8	3.60	2.5	2.5
-8.35	7.38	15.73	51	142.8	5.47	3.8	3.7
-6.35	9.33	15.68	50	140.0	8.57	6.1	6.0
-4.35	11.23	15.58	50	140.0	13.27	9.5	9.2
-2.35	12.93	15.28	48	134.4	19.63	14.6	14.2
-1.35	13.64	14.99	46	128.8	23.12	18.0	17.4
-0.35	14.16	14.51	44	123.2	26.06	21.2	20.4
0.65	14.53	13.88	43	120.4	28.38	23.6	22.6
1.65	14.77	13.12	42	117.6	29.99	25.5	24.3
2.65	14.93	12.28	40	112.0	31.12	27.8	26.1

Table 9. Measured power performance of ARL23M425 at 3.3 V.

433 MHz	Package E	ARL23 ARLTILE2 TQPED				3.3V ; 53 mA			
Pin(SG)	**Pout(PM)**	**Pin(corr)**	**Pout(corr)**	**Gain**	**I1(3.3V)**	**PDC(mw)**	**Pout(mw)**	**Drn Eff**	**PAE**
-15.0	0.61	-15.35	0.61	15.96	53	174.9	1.15	0.7	0.6
-10.0	5.58	-10.35	5.58	15.93	53	174.9	3.61	2.1	2.0
-8.0	7.40	-8.35	7.40	15.75	53	174.9	5.50	3.1	3.1
-6.0	9.35	-6.35	9.35	15.70	52	171.6	8.61	5.0	4.9
-4.0	11.28	-4.35	11.28	15.63	52	171.6	13.43	7.8	7.6
-2.0	13.13	-2.35	13.13	15.48	51	168.3	20.56	12.2	11.9
-1.0	13.98	-1.35	13.98	15.33	50	165.0	25.00	15.2	14.7
0.0	14.69	-0.35	14.69	15.04	49	161.7	29.44	18.2	17.6
1.0	15.20	0.65	15.20	14.55	48	158.4	33.11	20.9	20.2
2.0	15.56	1.65	15.56	13.91	47	155.1	35.97	23.2	22.3
3.0	15.82	2.65	15.82	13.17	45	148.5	38.19	25.7	24.5
4.0	15.99	3.65	15.99	12.34	44	145.2	39.72	27.4	25.8

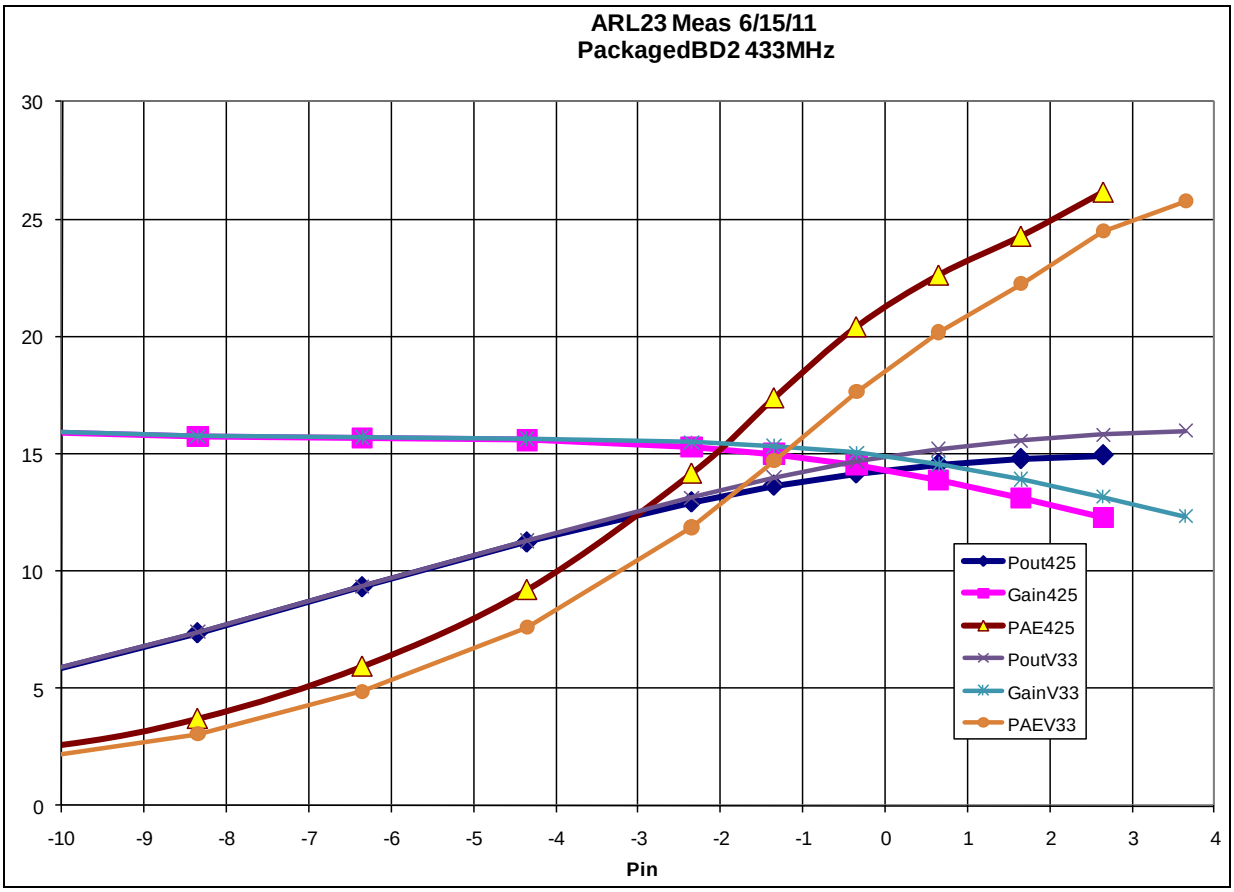

Figure 26. Plot of the gain, output power, and PAE of ARL23M425 at 2.8 and 3.3 V.

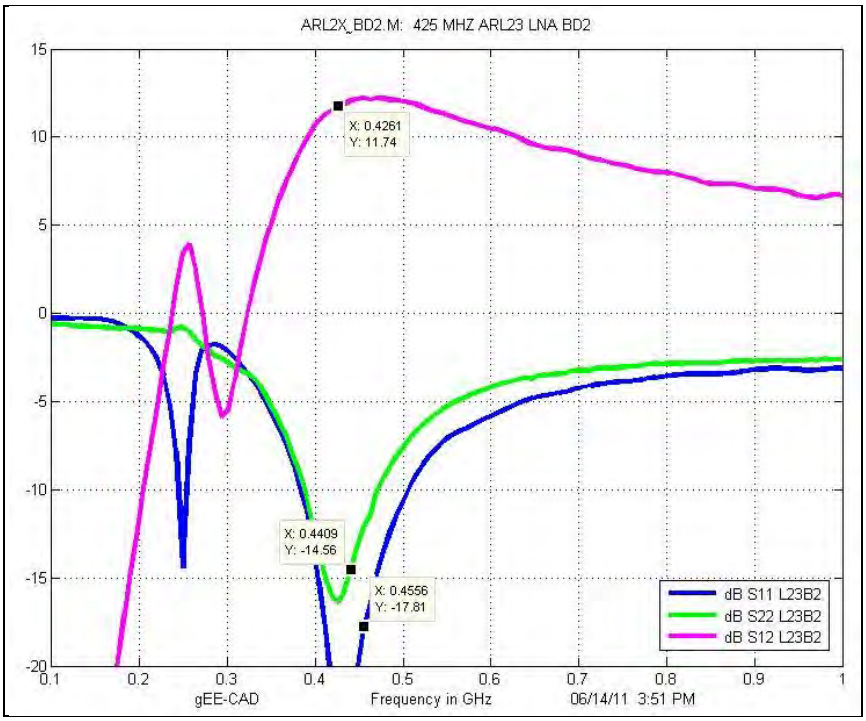

Figure 27. Measured S-parameters of the ARL23M425 receive state (2.8 V 51 mA).

Table 10. Measured noise figure and gain of ARL23M425 (2.8 V).

LNA		
Freq(MHz	Gain	NF
400.0	10.77	4.79
450.0	12.78	5.82
500.0	12.23	5.89
550.0	11.55	5.65
600.0	10.99	5.33
650.0	9.78	4.76

- ARL24DB—This dual-band design contains a BPSK modulator for 425 or 900 MHz, the broadband 50/75-mW PA for 2.8/3.6 V, a broadband moderate DC power consumption LNA, and a TR switch using positive voltage control inputs with negative threshold depletion PHEMTs. This design is intended to operate at either the 425 or 900 MHz frequency bands.

Figure 28 shows the measured S-parameter performance of the test board with ARL24DB at 2.8 V in the two transmit states of the BPSK modulator. Power performance of the design at 2.8 and 3.3 V for the 433-MHz band is shown in tables 11 and 12 along with a plot of this data in figure 29. Power performance of the design at 2.8 and 3.3 V for the 915-MHz band is shown in tables 13 and 14 along with a plot of this data in figure 30. Figure 31 shows the measured S-

parameter performance of the test board with ARL24DB at 2.8 V in the receive state along with a summary of the LNA's noise figure and gain in table 15.

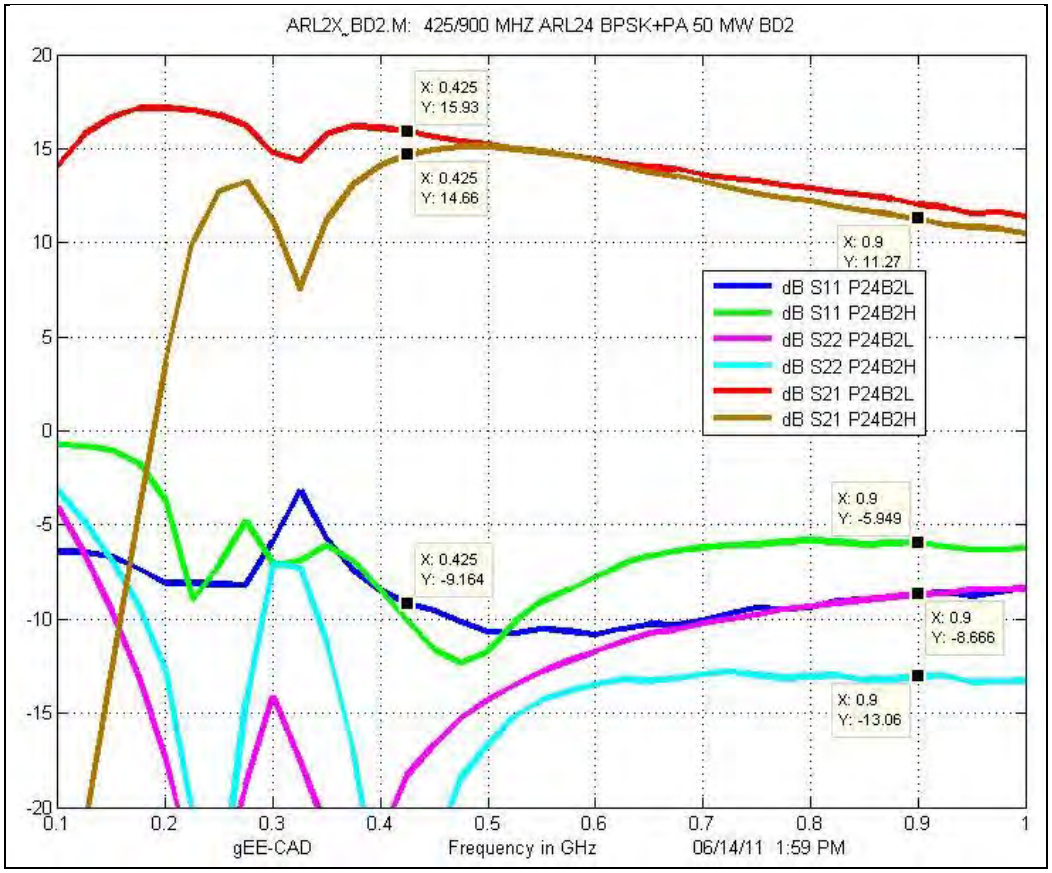

Figure 28. Measured S-parameters of the ARL24DB transmit states (2.8 V, 52 mA).

Table 11. Measured power performance of ARL24DB at 2.8 V and 433 MHz.

Uses BB LNA from ARLTILE1							
0.35 dB offset at input for 433 MHz				Includes LNA current			
ARL24DB ARLTILE2 TQPED				2.8V ; 52 mA			
Pin(corr)	**Pout(corr)**	**Gain**	**I1(2.8V)**	**PDC(mw)**	**Pout(mw)**	**Drn Eff**	**PAE**
-15.35	0.37	15.72	52	145.6	1.09	0.7	0.7
-10.35	5.34	15.69	52	145.6	3.42	2.3	2.3
-8.35	7.33	15.68	52	145.6	5.41	3.7	3.6
-6.35	9.27	15.62	51	142.8	8.45	5.9	5.8
-4.35	11.17	15.52	51	142.8	13.09	9.2	8.9
-2.35	12.90	15.25	49	137.2	19.50	14.2	13.8
-1.35	13.61	14.96	48	134.4	22.96	17.1	16.5
-0.35	14.14	14.49	46	128.8	25.94	20.1	19.4
0.65	14.50	13.85	45	126.0	28.18	22.4	21.4
1.65	14.74	13.09	44	123.2	29.79	24.2	23.0
2.65	14.91	12.26	43	120.4	30.97	25.7	24.2

Table 12: Measured power performance of ARL24DB at 3.3 V and 433 MHz

433 MHz	Package BD2	ARL24DB ARLTILE2 TQPED				3.3V ; 54 mA			
Pin(SG)	**Pout(PM)**	**Pin(corr)**	**Pout(corr)**	**Gain**	**I1(3.3V)**	**PDC(mw)**	**Pout(mw)**	**Drn Eff**	**PAE**
-15.0	0.37	-15.35	0.37	15.72	54	178.2	1.09	0.6	0.6
-10.0	5.35	-10.35	5.35	15.70	54	178.2	3.43	1.9	1.9
-8.0	7.34	-8.35	7.34	15.69	54	178.2	5.42	3.0	3.0
-6.0	9.28	-6.35	9.28	15.63	53	174.9	8.47	4.8	4.7
-4.0	11.20	-4.35	11.20	15.55	53	174.9	13.18	7.5	7.3
-2.0	13.05	-2.35	13.05	15.40	52	171.6	20.18	11.8	11.4
-1.0	13.91	-1.35	13.91	15.26	52	171.6	24.60	14.3	13.9
0.0	14.63	-0.35	14.63	14.98	51	168.3	29.04	17.3	16.7
1.0	15.15	0.65	15.15	14.50	50	165.0	32.73	19.8	19.1
2.0	15.50	1.65	15.50	13.85	49	161.7	35.48	21.9	21.0
3.0	15.76	2.65	15.76	13.11	48	158.4	37.67	23.8	22.6
4.0	15.95	3.65	15.95	12.30	48	158.4	39.36	24.8	23.4

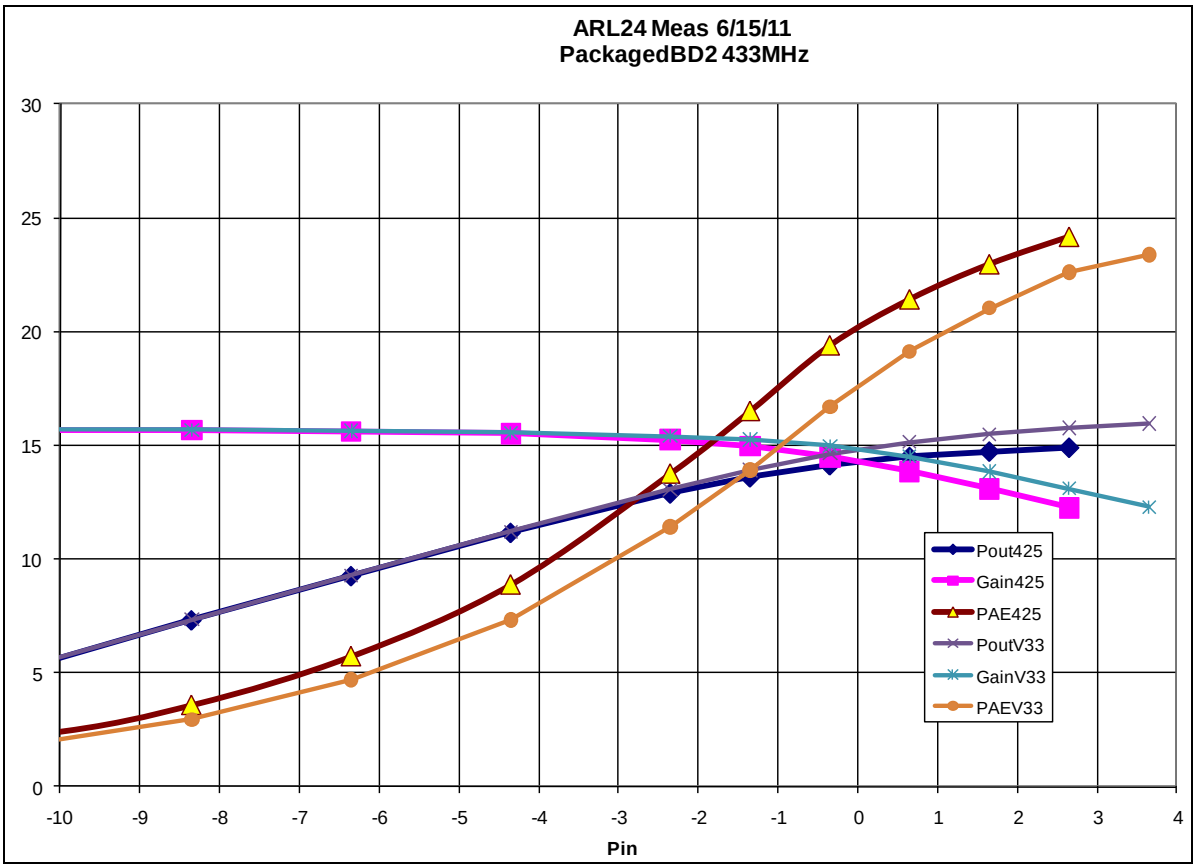

Figure 29. Plot of the gain, output power, and PAE of ARL24DB at 2.8 V, 3.3 V, and 433 MHz.

Table 13. Measured power performance of ARL24DB at 2.8 V and 915 MHz.

0.5 dB offset at input for 915 MHz				Includes LNA current			
ARL24DB ARLTILE2 TQPED				2.8V ; 52 mA			
Pin(corr)	**Pout(corr)**	**Gain**	**I1(2.8V)**	**PDC(mw)**	**Pout(mw)**	**Drn Eff**	**PAE**
-15.50	-3.58	11.92	52	145.6	0.44	0.3	0.3
-10.50	1.40	11.90	52	145.6	1.38	0.9	0.9
-8.50	3.28	11.78	52	145.6	2.13	1.5	1.4
-6.50	5.26	11.76	52	145.6	3.36	2.3	2.2
-4.50	7.23	11.73	52	145.6	5.28	3.6	3.4
-2.50	9.18	11.68	51	142.8	8.28	5.8	5.4
-0.50	11.10	11.60	51	142.8	12.88	9.0	8.4
1.50	12.84	11.34	50	140.0	19.23	13.7	12.7
2.50	13.56	11.06	48	134.4	22.70	16.9	15.6
3.50	14.09	10.59	47	131.6	25.64	19.5	17.8
4.50	14.44	9.94	46	128.8	27.80	21.6	19.4
5.50	14.66	9.16	45	126.0	29.24	23.2	20.4
6.50	14.81	8.31	45	126.0	30.27	24.0	20.5

Table 14. Measured power performance of ARL24DB at 3.3 V and 915 MHz.

915 MHz	Package BD2	**ARL24DB ARLTILE2 TQPED**				3.3V ; 54 mA			
Pin(SG)	**Pout(PM)**	**Pin(corr)**	**Pout(corr)**	**Gain**	**I1(3.3V)**	**PDC(mw)**	**Pout(mw)**	**Drn Eff**	**PAE**
-15.0	-3.58	-15.50	-3.58	11.92	54	178.2	0.44	0.2	0.2
-10.0	1.39	-10.50	1.39	11.89	54	178.2	1.38	0.8	0.7
-8.0	3.27	-8.50	3.27	11.77	54	178.2	2.12	1.2	1.1
-6.0	5.25	-6.50	5.25	11.75	54	178.2	3.35	1.9	1.8
-4.0	7.22	-4.50	7.22	11.72	54	178.2	5.27	3.0	2.8
-2.0	9.17	-2.50	9.17	11.67	53	174.9	8.26	4.7	4.4
0.0	11.10	-0.50	11.10	11.60	53	174.9	12.88	7.4	6.9
2.0	12.91	1.50	12.91	11.41	53	174.9	19.54	11.2	10.4
3.0	13.73	2.50	13.73	11.23	52	171.6	23.60	13.8	12.7
4.0	14.42	3.50	14.42	10.92	52	171.6	27.67	16.1	14.8
5.0	14.94	4.50	14.94	10.44	51	168.3	31.19	18.5	16.9
6.0	15.30	5.50	15.30	9.80	50	165.0	33.88	20.5	18.4
7.0	15.55	6.50	15.55	9.05	50	165.0	35.89	21.8	19.0

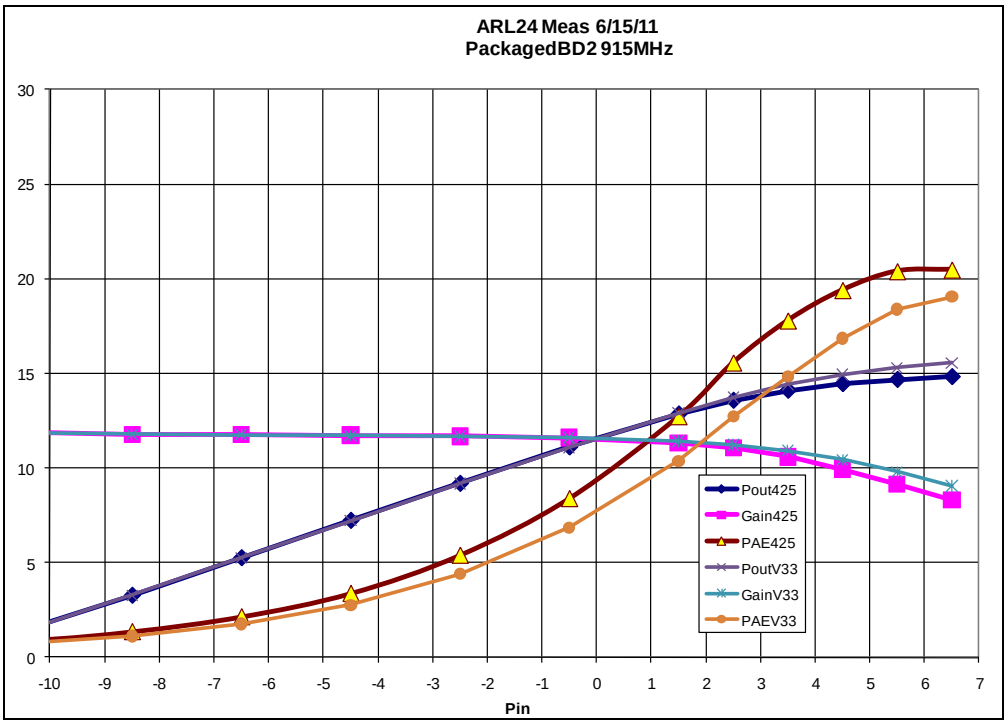

Figure 30. Plot of the gain, output power, and PAE of ARL24DB at 2.8 V, 3.3 V, and 915 MHz.

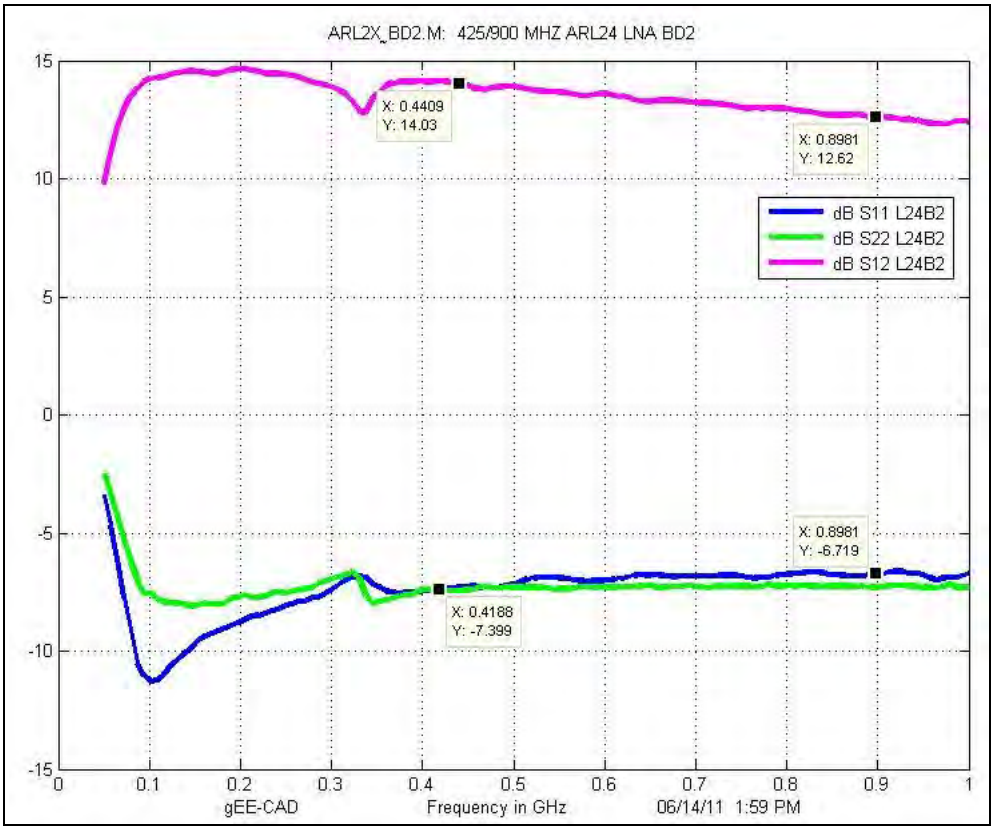

Figure 31. Measured S-parameters of the ARL24DB receive state (2.8 V 52 mA).

Table 15. Measured noise figure and gain of ARL24DB (2.8 V).

LNA		
Freq(MHz)	**Gain**	**NF**
400.0	15.01	6.34
450.0	14.50	6.42
500.0	13.85	6.15
550.0	13.97	6.06
600.0	14.05	6.05
650.0	13.94	5.95
700.0	13.64	5.87
750.0	**13.51**	**5.56**
800.0	**13.73**	**5.97**
850.0	13.35	5.87
900.0	12.96	5.80
950.0	13.26	5.30

Overall, the performance of the Booster ICs in the test boards yields comparable performance to previous measurements. It is noted that the noise figures seem higher. There could be several factors causing a higher measurement here. Pullup resistors are used for the control signals, which tie to the input DC power supply. The power supply also acts as a reference for the transmit/receive switch to operate with positive control voltages while using depletion (negative threshold) PHEMT switches. Possibly the DC power supplies need additional decoupling capacitors, or filtering, for both of these concerns. Thirdly, for the measurements of the LNA noise figure, both the PA and LNA are powered up simultaneously. Since the BPSK modulators are not used for testing with the RF access point, any of the four designs can be used for both the 433- and 915-MHz RF access point boards as long as the BPSK modulator is in the high pass state.

10. Wireless Communications Testing of Booster ICs with the RF Access Point

The concept of the Booster IC is illustrated in figure 32 where the COTS transceiver is shown as a TI CC1110 part followed by an integrated matching IC to reduce SWAP, followed by the active RF front end Booster IC to enhance performance. Both the integrated matching and the active portion of the RF Booster IC could be combined into a single die and/or package, but are functionally shown separately. The matching and active ICs were fabricated as separate die in the 2nd pass ARL GaAs tile for the Booster IC.

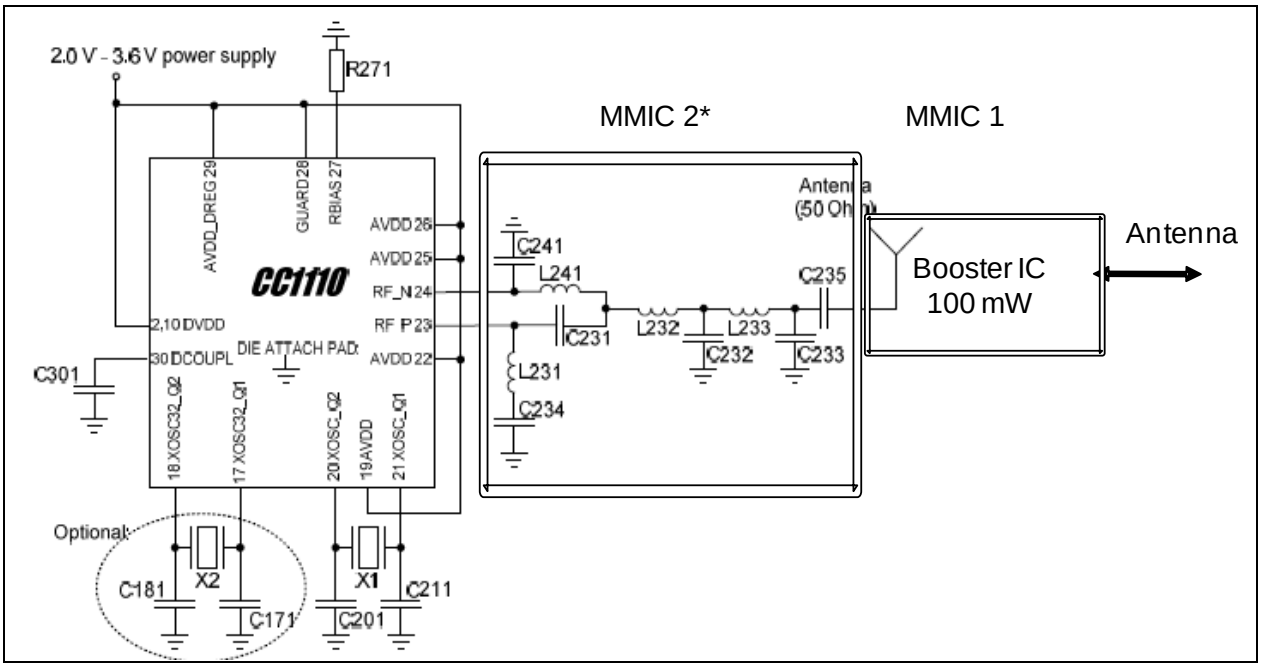

Figure 32. COTS RFIC performance enhanced with the matching IC and RF active booster IC.

For testing the Booster IC in a system, the RF access point of the TI Chronos development kit (figure 33) provides bidirectional wireless communication between a computer and the Chronos sports watch. Modified RF access point boards for 433- and 915-MHz operation were modified to demonstrate a system using the Booster IC.

Figure 33. TI Chronos wireless communications development kit.

As mentioned previously, first a small UFL RF connector replaced the chip antenna on one RF access point board to allow modular testing. A second RF access point was modified by replacing its discrete matching components with a single integrated passive matching IC, followed by a small UFL RF connector. Because of the need for two or three discrete lumped element matching components to match the antenna to 50 ohms, these two modified boards do

not represent an equivalent —apples to apples" comparison. It might appear that the matching circuit provides better output power rather than just integration and improved SWAP. The output power of the RF access point plus ARL29M425 matching circuit was about 5.9 dBm measured with the N1912 Agilent Power Sensor with a GSM mode preset. This modified board was then used to drive the test boards for the active Booster ICs. Since the power level of the COTS RFIC was pre-programmed to a relatively high output level, SMA barrel attenuators were used to set the input drive level appropriately. Figure 34 shows the USB RF access point board connected to an active Booster IC PC board for bidirectional system tests. In the figure, a wireless transmission from the watch is received at the monopole antenna, attenuated 20 dB, then feeds through the receive path of the Booster IC board. For testing the transmit —heart rate pulse," the RF access board would connect to the input SMA (right/top) of the Booster IC test board. Following are oscilloscope images of the 433-MHz tests along with a table summarizing the input and output drive level of each active Booster IC design and effective large signal gain at 3-dB compression. To attain the appropriate drive level, a 3-dB attenuator was used at the input of ARL21M425, a 2-dB attenuator was used for ARL22M425, and 4-dB attenuators were used for ARL23M425 and ARL24DB. In the table, the 20-dB attenuator used at the output of each Booster IC has been compensated for, but note that the voltages in the oscilloscope plots following are a factor of 10 smaller in magnitude than the actual signal (20 dB).

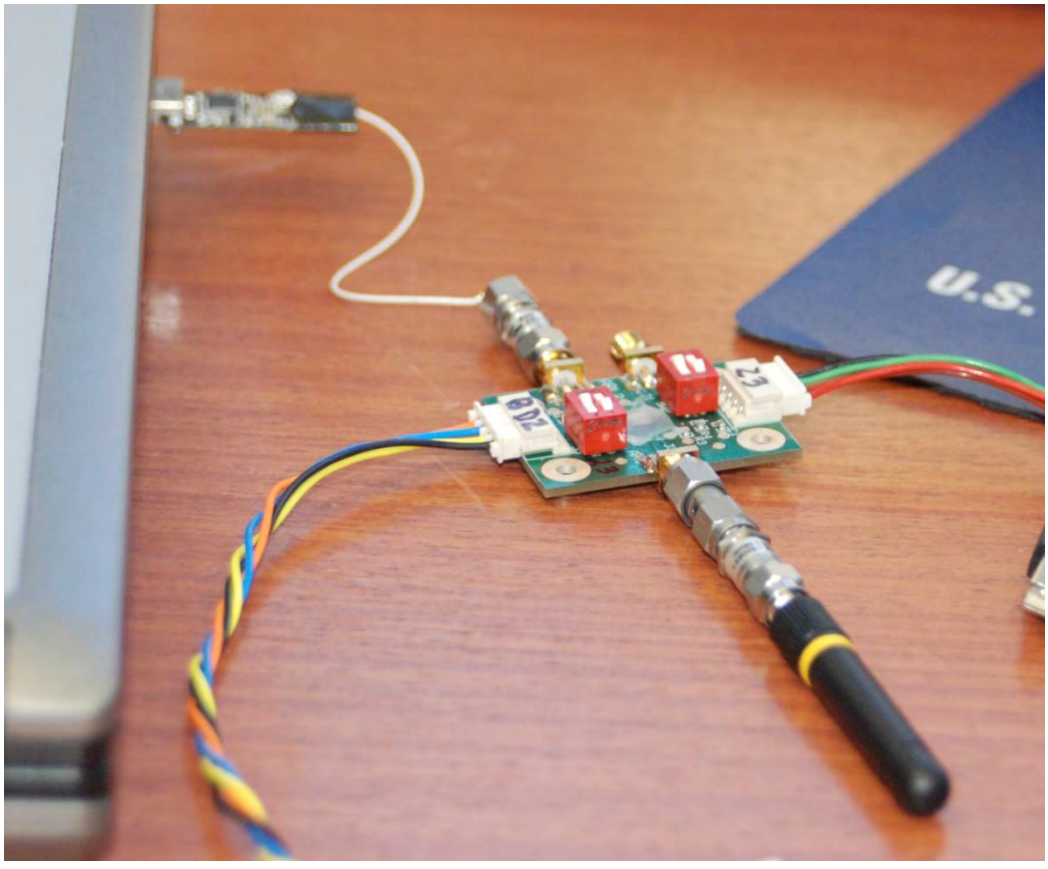

Figure 34. Booster IC PC board with the RF access point for the system test.

An oscilloscope with a 50-MHz, 50-ohm input was used to look at the 433-MHz RF access point pulses during emulation of a wireless heart rate monitor. Figure 35 shows the RF access point output with only a 50-ohm RF connector in place of the chip antenna. This may be poorly matched to 50 ohms explaining the low –3.3 dBm output (~260 mV p-p). With the ARL29M425 IC providing proper matching, the output amplitude is 5.9 dBm (~800 mV p-p) for the 486 µs long pulse (figure 36).

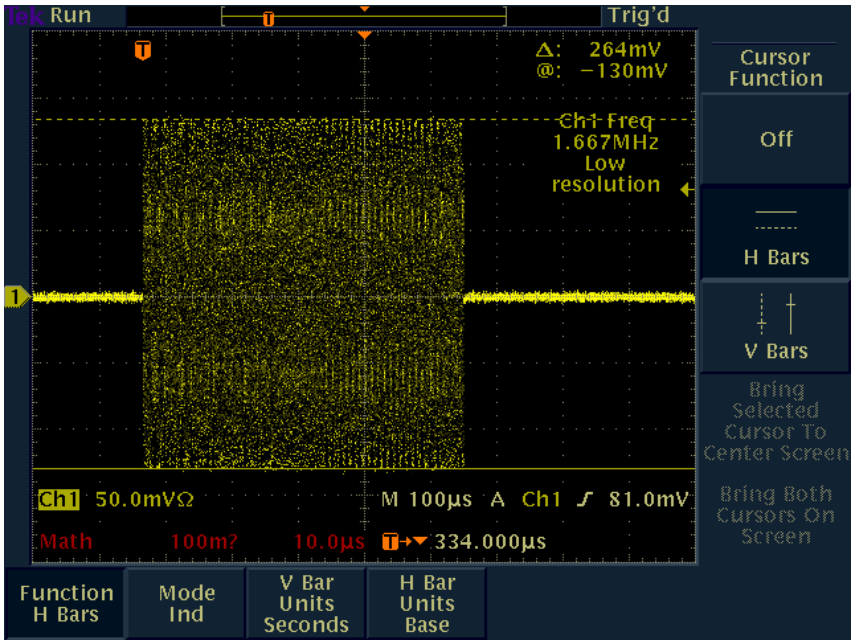

Figure 35. TI RF access point heart rate pulse (no chip antenna).

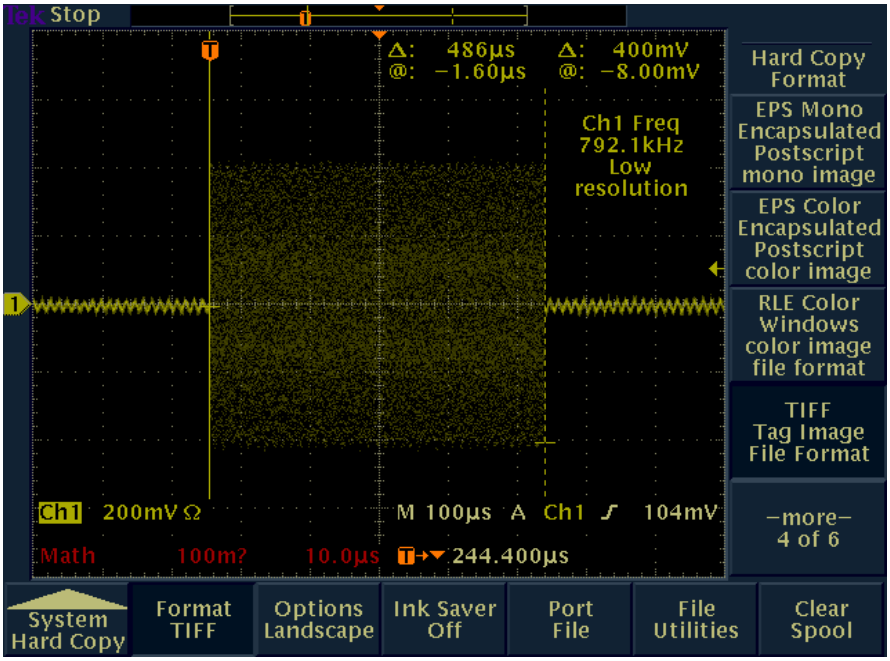

Figure 36. TI RF access point heart rate pulse with the ARL29M425 IC (matching).

The matched 433-MHz RF access point board with the ARL29M425 matching IC was used to drive each of the active Booster IC test boards. Oscilloscope plots of the four active designs, ARL21M425, ARL22M425, ARL23M425, and ARL24DB are shown in figures 37, 38, 39, and 40. While a similar test was done with a 915-MHz RF access point board and the ARL26DB matching IC, the oscilloscope plots are only available with the 433-MHz tests. Amplitudes after the 20-dB attenuator are 291, 244, 205, and 212 mV (p-p) corresponding to the P3dB output levels of ARL21, 22, 23, and 24 active Booster ICs (table 16).

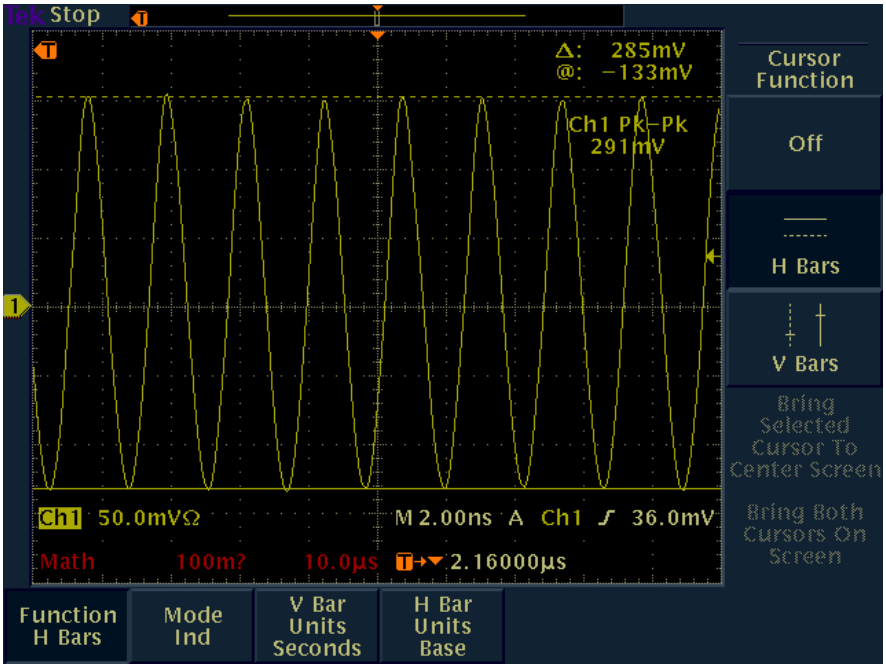

Figure 37. 433-MHz RF access point with ARL29M425 IC and ARL21M425 (291 mV p-p).

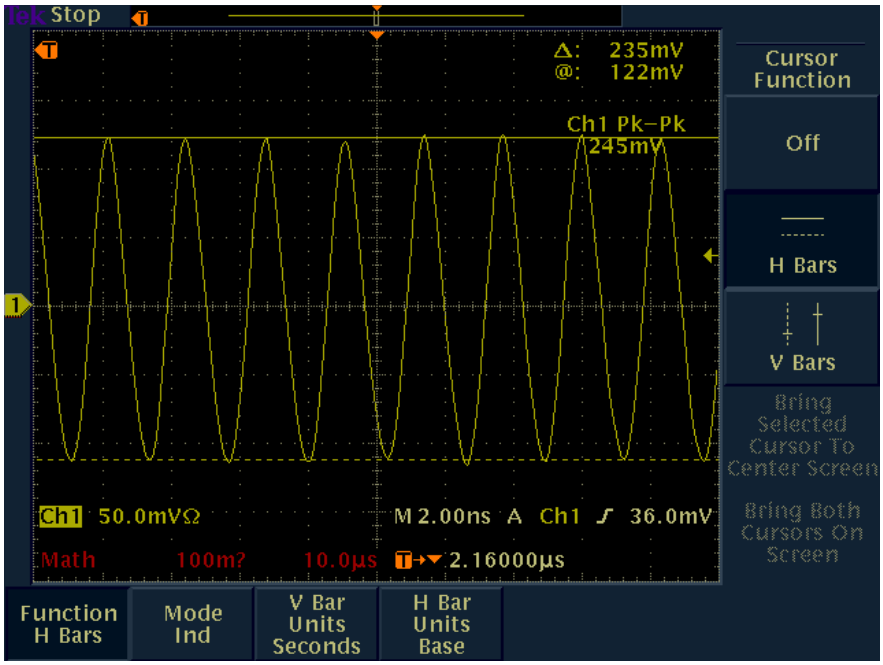

Figure 38. 433-MHz RF access point with ARL29M425 IC and ARL22M425 (245 mV p-p).

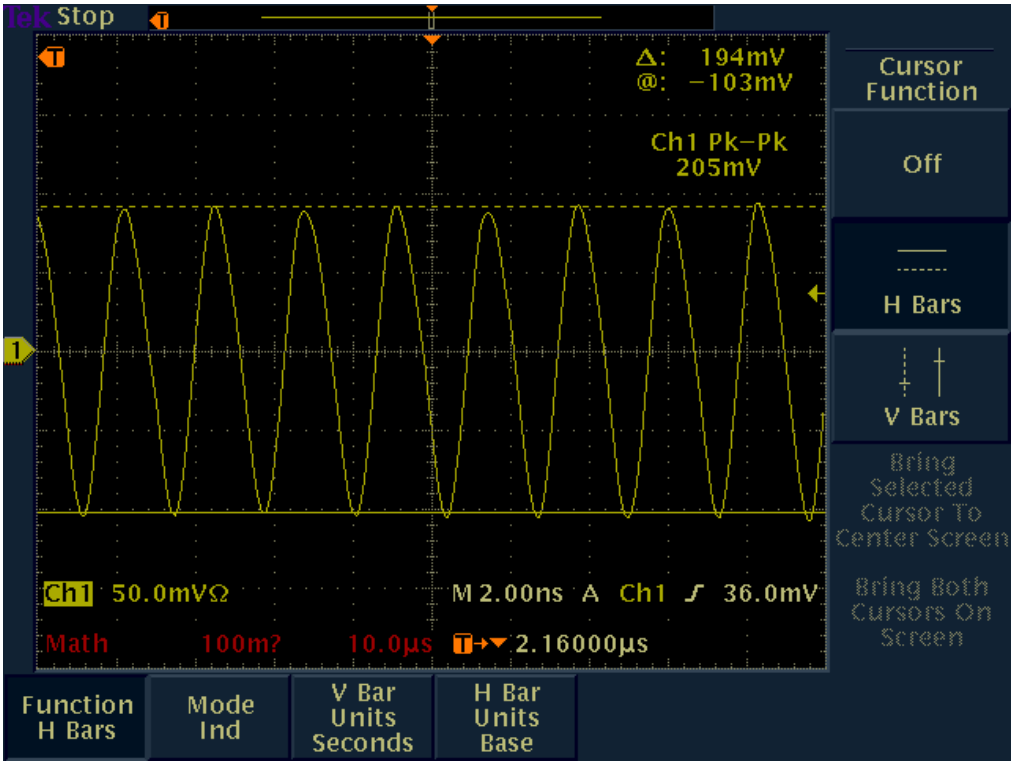

Figure 39. 433-MHz RF access point with ARL29M425 IC and ARL23M425 (205 mV p-p).

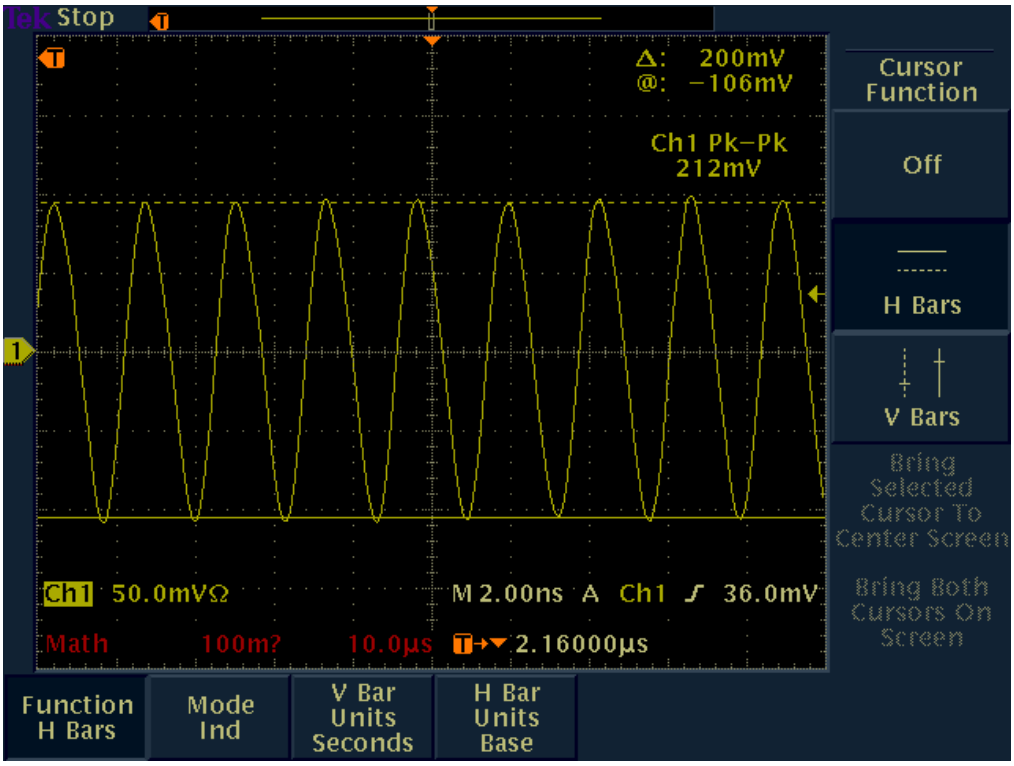

Figure 40. 433-MHz RF access point with ARL29M425 IC and ARL24DB (212 mV p-p).

Table 16. Measured output power and gain of the booster IC with a 433-MHz RF access point.

Design	DC Bias	Pin (dBm)	LS Gain (P3dB)	Pout (dBm)
RFAcc+ARL29		5.9		
ARL21M425	2.8V, 84 mA	2.9	15.1	18.0
ARL22M425	2.8V, 43 mA	3.9	12.1	16.0
ARL23M425	2.8V, 51 mA	1.9	11.9	14.8
ARL24DB	2.8V, 52 mA	1.9	11.9	14.8

The matched 915-MHz RF access point board with the ARL26DB matching IC was used to drive each of the active Booster IC test boards. The power meter was used to measure the outputs at 915 MHz. For the narrowband designs, the BPSK modulator was put in the high pass state to have sufficient gain at 915 MHz. ARL24 is not shown but uses the same power amplifier design as ARL23, so its performance should have been comparable. Since E-mode switches were used in the dual-band switched matching circuits of the ARL26DB IC, the large signal output of the RF access point is overdriven and clipping in amplitude skewing the results for this test. With additional effort, the RF access point could be programmed to reduce its output power level to keep from clipping in the dual-band matching IC, but then the output levels would be insufficient to drive the active Booster ICs. A redesign would likely replace the E-mode switches with D-mode switches to handle the higher RF power but there may be other tradeoffs at the system level. As a proof of concept, the current design was sufficient to show dual-band or broadband capability with both a broadband matching IC for the COTS RFIC and a

broadband Booster IC (ARL24DB) for enhanced RF performance. Table 17 summarizes the test results at 915 MHz.

Table 17. Measured output power and gain of the booster IC with a 915-MHz RF access point.

Design	DC Bias	Pout (dBm)
RFAcc+ARL26	1.0 V	–1.1
ARL21M425	2.8 V, 84 mA	15.2
ARL22M425	2.8 V, 43 mA	13.2
ARL23M425	2.8 V, 51 mA	14.0

A system level test of the 2nd pass Booster IC designs was performed using the TI Chronos development kits at 433 and 915 MHz. Passive circuits were designed in the 2nd pass Booster IC GaAs tile to demonstrate improved SWAP by integrating the discrete lumped element matching circuits required by COTS wireless transceiver ICs and also to demonstrate a broadband or dual-band capability by adding PHEMT switches. One of the passive circuits, ARL29M425, was used with the RF access point at 433 MHz to demonstrate the improved SWAP by integrating the matching circuit required by the TI CC11XX RFIC. Another passive circuit, ARL26DB, was used with the RF access point at 915 MHz to demonstrate the ability to change bands using an integrated matching circuit with PHEMT switches.

For the transmit test, the amplified heart rate pulse was successfully received by the sports watch. Output levels were measured to verify the gain and performance enhancement achieved by the active Booster ICs. For the receive mode, the development kit was used to receive accelerometer data from the sports watch using the receive path of the active Booster ICs. The receive test was a qualitative test, not a quantitative measurement.

The TI Chronos development kits provided an easy, inexpensive means to test the RF performance enhancements of the GaAs Booster ICs using modified RF access point boards and the existing software. It demonstrates the ease of plugging in the Booster IC for improved performance without negating the existing IP and development for the core COTS RFIC.

11. Wireless Tag Designs using Booster ICs with the TI CC11XX RFIC

The TI Chronos development kits provided a demonstration of a wireless system with enhanced system performance using an RF frontend optimized in GaAs and easily inserted into a COTS-based RFIC system. The advantages of digital integration, software development, and IP for the COTs Si RFIC are maintained while the performance advantages of other integrated circuit processes can be used to optimize the system-level RF performance. While the passive matching circuits of the Booster IC and active amplifiers were demonstrated at a module, or board level,

all of the components could be integrated into a small compact wireless board or module. Following are two-sided board layouts based on the RF access point that could be fabricated to demonstrate an integrated board with the Booster ICs. Since the capability was already demonstrated sufficient to prove out the system-level concepts of the Booster IC, it is not currently planned for fabrication, but could be. The first design (#1) adds the ARL29M425 matching circuit to the RF access point design. The preprogrammed parts of an existing RF access point board could be removed and added to this design along with a packaged ARL29M425 for an integrated demonstration. This layout also adds a connector for programming the CC11XX RFIC, which was not included on the original RF access point board. The second design (#2) is similar to the first but now adds the ARL21M425 (or 22/23/24) active Booster IC to the RF access point design. Figure 41 is a schematic of the first wireless design while figures 42 and 43 are the top and bottom sides of the PC board layout. Likewise, figure 44 is a schematic of the second wireless design while figures 45 and 46 are the top and bottom sides of the second PC board layout.

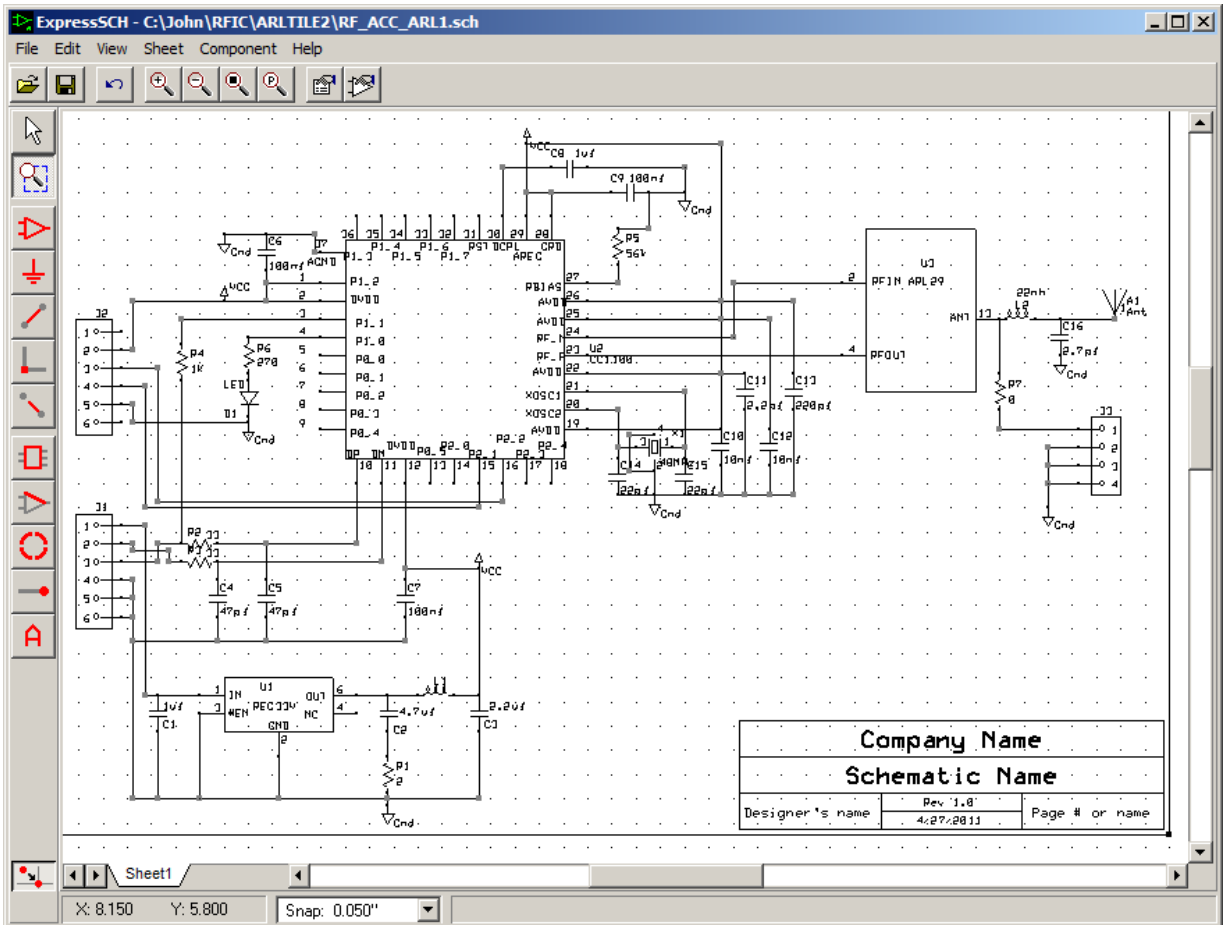

Figure 41. Schematic of the wireless system with the TI CC11XX and the ARL29M425 IC.

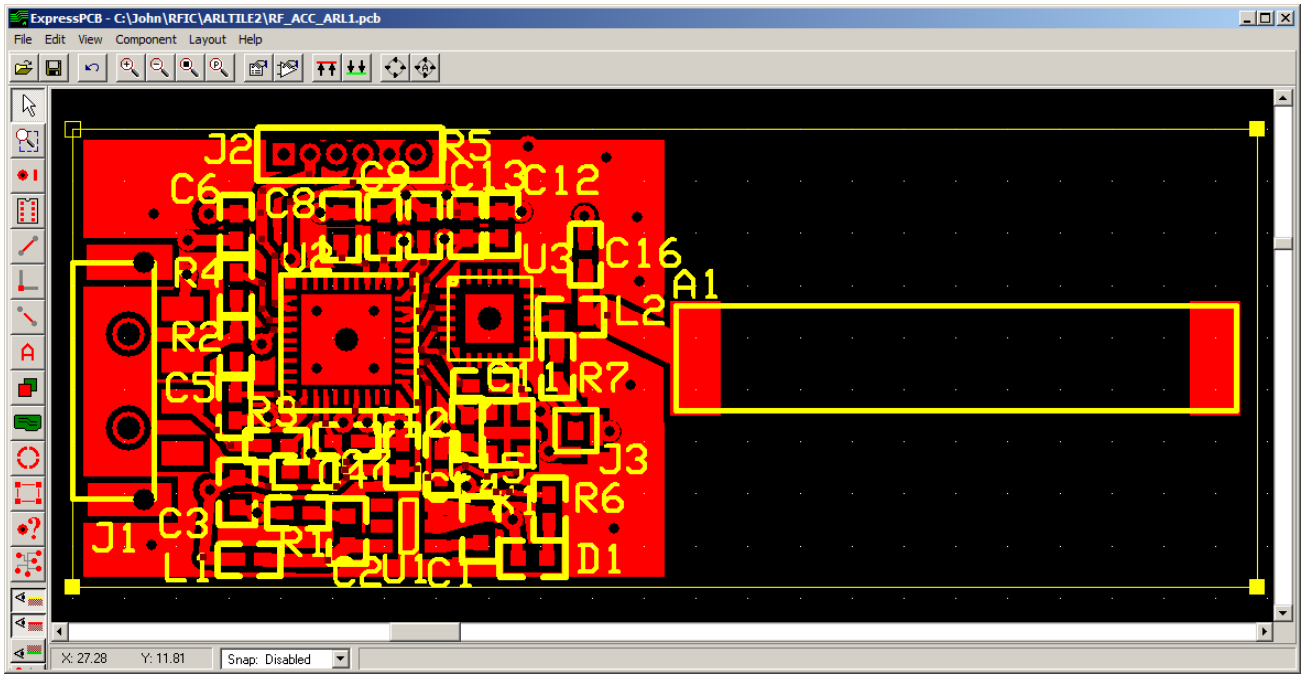

Figure 42. Top side PC board layout of the first wireless system (CC11XX + ARL29M425).

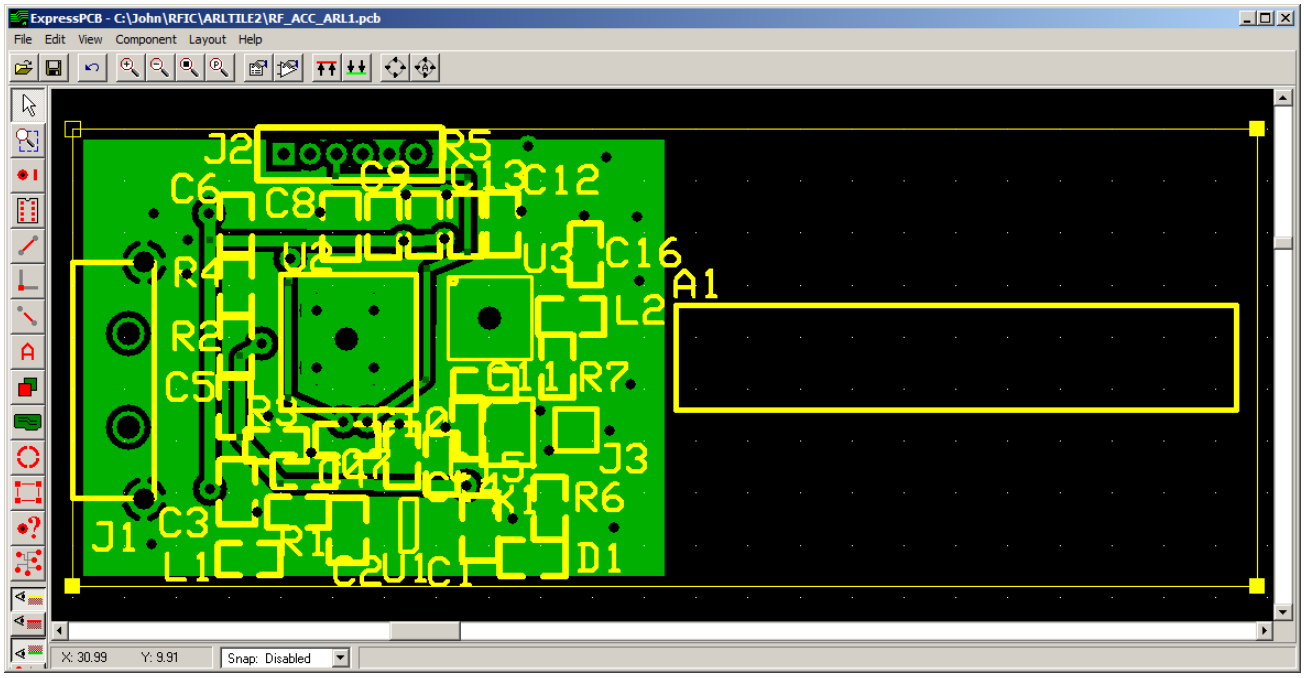

Figure 43. Bottom side PC board layout of the first wireless system (CC11XX + ARL29M425).

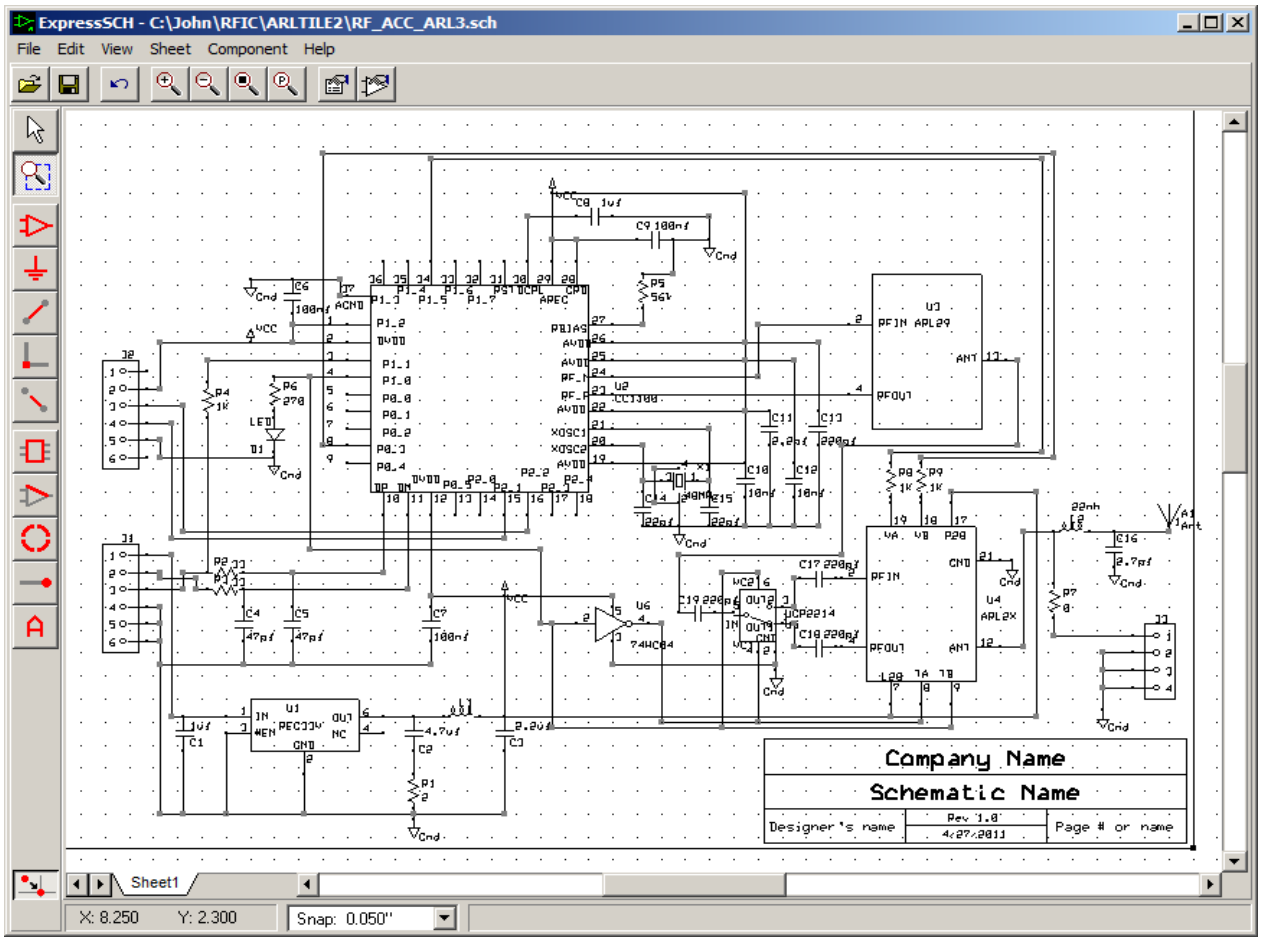

Figure 44. Schematic of the second wireless system adding the active booster ARL2X IC.

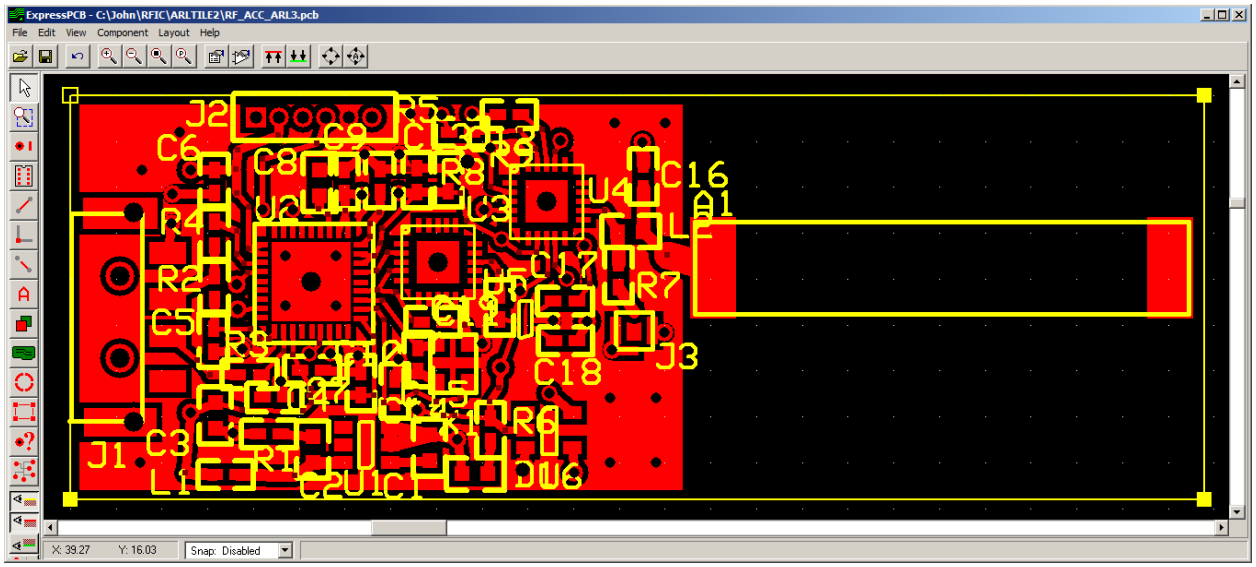

Figure 45. Top side PC board layout of the second wireless system (ARL2X).

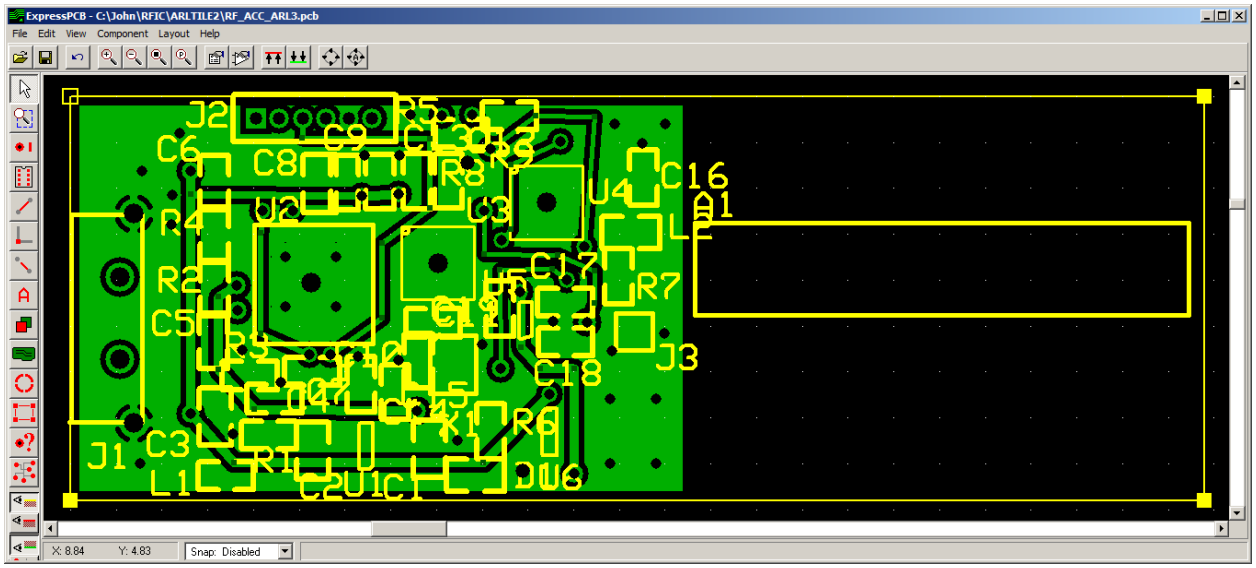

Figure 46. Bottom side PC board layout of the second wireless system (ARL2X).

12. Conclusion

A system-level test of the 2nd pass Booster IC designs was performed at ARL. The designs are also being integrated into a tag system by an outside system integrator. Tests were performed by the system integrator demonstrating successful transmission using a 1st pass Booster IC design. The same system integrator is developing a tag using the 2nd pass Booster IC designs for full bidirectional communications. That effort will be documented separately.

This demonstration of a wireless system using the 2nd pass Booster ICs used TI Chronos development kits at 433 and 915 MHz. Two of the passive Booster IC designs demonstrated the integration of many discrete matching elements for improved SWAP and a dual-band matching circuit for a sub-1 GHz COTS RFIC. The four active Booster ICs consist of one design optimized for 100 mW of output power with a 2.8-V supply, another for 50 mW of output power with a 2.8-V supply, a robust design for 2.8- to 3.6-V supply (or higher), and a dual-band design. All four active designs were successfully tested for bidirectional communications using the 433 and 915 MHz Chronos development kits.

The TI Chronos development kits provided an easy, inexpensive means to test the RF performance enhancements of the GaAs Booster ICs using modified RF access point boards and the existing software for the transmission and reception of data to the wireless watch. It demonstrates the ease of plugging in the Booster IC for improved performance without negating the existing IP and development of the base COTS RFIC.

The concept of custom IC design for enhanced RF performance can be extended to other frequencies, wireless communications systems, and power levels. Combinations of different IC technologies can be integrated to take advantage of the optimal characteristics of each technology. For instance, a gallium nitride (GaN) IC Booster IC could further extend the current low frequency applications from hundreds of mW of output power to several W of output power (figure 47). Our Soldiers do not need to rely solely on COTS parts to determine the limitations of electronic systems, judicious application of combinations of IC technologies can be used to surpass what might seem like limitations in current technologies or available COTS parts.

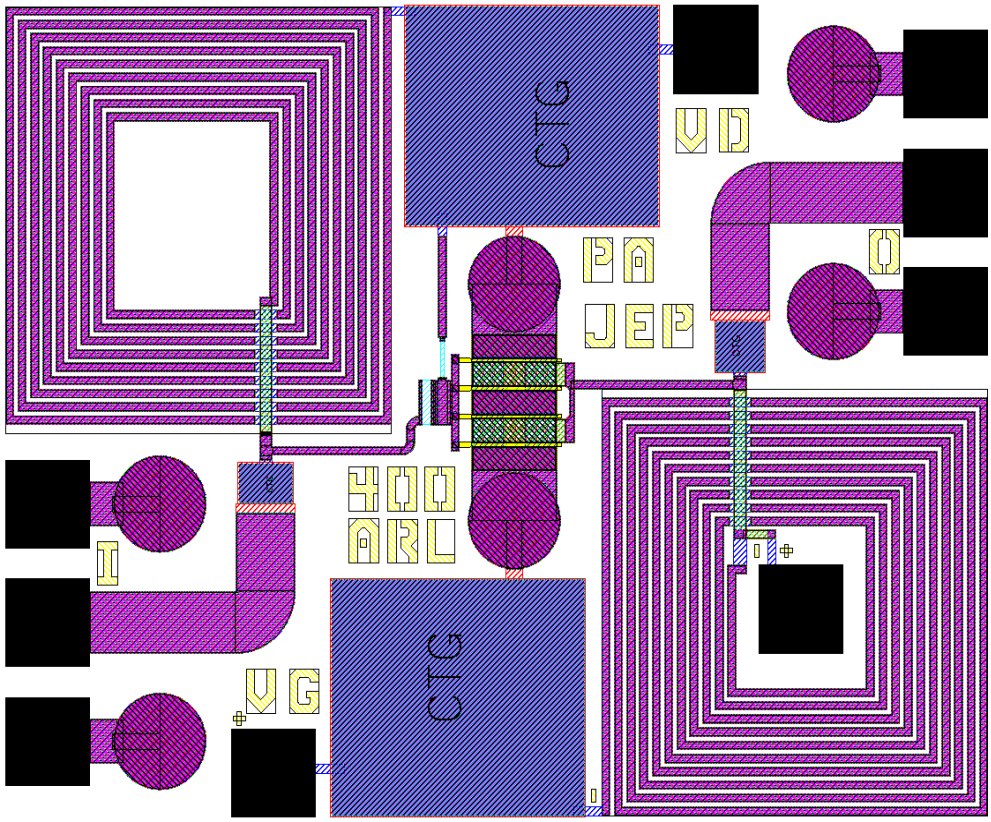

Figure 47. Layout of a 2-W GaN UHF PA (~1 mm^2).

The following is a summary of the custom Booster IC for enhanced RF performance:

- Uses superior RF performance of GaAs* to enhance a Si COTS RFIC wireless system.
- *Increased operating range*: The current designs are optimized for CC11XX targets a 10 times increase in transmit power (10 mW maximum for CC11XX, 100 mW ARL21M425 Booster IC transmit power).
- *Improved sensitivity*: The noise figure of GaAs LNAs is superior to Si. The advantage varies depending on COTS RFIC and optimization of Booster IC design.

* It could use GaN or other appropriate technology.

- *Simple Insertion into existing RFIC system*: This design is intended to be easily inserted into the RF connection between a COTS RFIC and antenna. It does not negate IP and software development of the base RFIC system.
- *Improved SWAP*: This is gained by integrating matching circuit elements into an IC (ARL29M425).
- *Ability to make dual-band or broadband systems*: Good switch devices in GaAs make it possible to broadband match circuits for dual-band or broadband use (ARL26DB).

13. References

1. Mitchell, G.; Penn, J. *Preliminary Gallium Arsenide (GaAs) Integrated Circuit Design for Radio Frequency Booster Chips at 450, 900, and 2400 MHz*; ARL-TR-4970; U.S. Army Research Laboratory: Adelphi, MD, September 2009.

2. Penn, J. *GaAs Microwave Integrated Circuit Designs Submitted to TriQuint Semiconductor for Fabrication*; ARL-TN-0381; U.S. Army Research Laboratory: Adelphi, MD, December 2009.

3. Mitchell, G.; Penn, J. *Results of Bare Die Probing for RF Booster Chip at 400, 900, 2400 MHz*; ARL-TR-5170; U.S. Army Research Laboratory: Adelphi, MD, April 2010.

4. Penn, J. *Testing of GaAs Microwave Integrated Circuit Designs in QFN Packages*; ARL-TR-5131; U.S. Army Research Laboratory: Adelphi, MD, March 2010

5. Penn, J. *GaAs Microwave Integrated Circuit Designs Submitted to TriQuint Semiconductor for Fabrication (ARL Tile #2)*; ARL-TN-0404; U.S. Army Research Laboratory: Adelphi, MD, September 2010.

6. Penn, J. *Optimized (2nd Pass) Gallium Arsenide (GaAs) Integrated Circuit Radio Frequency (RF) Booster Designs for 425 MHz and Dual Band (425 and 900 MHz)*; ARL-TR-5396; U.S. Army Research Laboratory: Adelphi, MD, November 2010.

7. Penn, J. *Results of Bare Die Testing of Optimized (2nd Pass) Gallium Arsenide (GaAs) Integrated Circuit Radio Frequency (RF) Booster Designs for 425 MHz and Dual Band (425 and 900 MHz)*; ARL-TR-5465; U.S. Army Research Laboratory: Adelphi, MD, February 2011.

8. Penn, J. *Testing of Active Optimized (2nd Pass) Gallium Arsenide (GaAs) Integrated Circuit Radio Frequency (RF) Booster Designs for 425 MHz and Dual Band (425 and 900 MHz) in QFN Packages*; ARL-TR-5459; U.S. Army Research Laboratory: Adelphi, MD, February 2011.

List of Symbols, Abbreviations, and Acronyms

ARL	U.S. Army Research Laboratory
BPSK	binary phase shift keying
COTS	commercial off the shelf
DIP	dual inline package
D-mode	depletion mode
E-mode	enhancement mode
GaAs	gallium arsenide
GaN	gallium nitride
HP	high pass
IC	integrated circuit
LNA	low noise amplifier
LP	low pass
PA	power amplifier
PAE	power-added efficiency
PC	printed circuit
PHEMT	pseudomorphic high electron mobility transistor
QFN	quad flat no leads
RF	radio frequency
RFIC	radio frequency integrated circuit
Si	silicon
SWAP	size, weight, and power
TI	Texas Instruments
TR	transmit/receive
TTL	Tagging, Tracking, and Locating

UHF	ultra-high frequency
USB	universal serial bus

NO. OF COPIES	ORGANIZATION
1 (PDF only)	DEFENSE TECHNICAL INFORMATION CTR DTIC OCA 8725 JOHN J KINGMAN RD STE 0944 FORT BELVOIR VA 22060-6218
1	DIRECTOR US ARMY RESEARCH LAB IMNE ALC HRR 2800 POWDER MILL RD ADELPHI MD 20783-1197
1	DIRECTOR US ARMY RESEARCH LAB RDRL CIO LL 2800 POWDER MILL RD ADELPHI MD 20783-1197
1	DIRECTOR US ARMY RESEARCH LAB RDRL CIO MT 2800 POWDER MILL RD ADELPHI MD 20783-1197
11	DIRECTOR US ARMY RESEARCH LAB RDRL SER PAUL AMIRTHARAJ RDRL SER E ROMEO DEL ROSARIO GREG MITCHELL JAMES WILSON GLEN BIRDWELL ROB REAMS JOHN PENN (3 HCS) ED VIVEIROS RDRL SEG STEVE RAGER 2800 POWDER MILL RD ADELPHI MD 20783-1197
1	CERDEC I2WD RDER IWR CI BOB GROSS SUITE D 6240 GUARDIAN GATEWAY APG MD 21005
1	I2WD STEVE HAUGHT FT MONMOUTH NJ

INTENTIONALLY LEFT BLANK.